NASA CR-134612

DEVELOPMENT OF FINE-DIAMETER MULLITE FIBER

by

W. G. Long

THE BABCOCK & WILCOX COMPANY

Prepared for

NATIONAL AERONAUTICS & SPACE ADMINISTRATION

NASA Lewis Research Center
Contract NAS 3-16764
John P. Merutka, Project Manager

LRC 5467
August 1974

1. Report No. NASA-CR-134612	2. Government Accession No.	3. Recipient's Catalog No.
4. Title and Subtitle DEVELOPMENT OF FINE DIAMETER MULLITE FIBER		5. Report Date FEBRUARY 20, 1974 6. Performing Organization Code
7. Author(s) W. G. LONG		8. Performing Organization Report No. LRC-5467 10. Work Unit No.
9. Performing Organization Name and Address BABCOCK & WILCOX COMPANY REFRACTORIES DIVISION OLD SAVANNAH ROAD AUGUSTA, GEORGIA BABCOCK & WILCOX COMPANY RESEARCH & DEVELOPMENT DIVISION P. O. BOX 1260 LYNCHBURG, VIRGINIA		11. Contract or Grant No. NAS 3-16764 13. Type of Report and Period Covered CONTRACTOR REPORT
12. Sponsoring Agency Name and Address NATIONAL AERONAUTICS AND SPACE ADMINISTRATION WASHINGTON, D.C. 20546		14. Sponsoring Agency Code

15. Supplementary Notes

PROJECT MANAGER, JOHN P. MERUTKA, NASA LEWIS RESEARCH CENTER, CLEVELAND, OHIO

16. Abstract

This report contains the results of a research program to develop and evaluate mullite fiber with a mean diameter under two microns. The two micron fiber is produced by a blowing process at room temperature from a low viscosity (10-25 poise) solution. The blown fiber was evaluated for dimensional stability in thermal cycling to 1371C, and was equivalent to the 5 micron spun B&W mullite fiber. An additive study was conducted to evaluate substitutes for the boron. Three levels of chromium, lithium fluoride, and magnesium were added to the standard composition in place of boron and the fiber produced was evaluated for chemical and dimensional stability in thermal cycling to 1371C. The magnesium was the most chemically stable, but the chrome additive imparted the best dimensional stability.

17. Key Words (Suggested by Author(s))	18. Distribution Statement
CERAMIC FIBER THERMAL PROPERTIES CRYSTAL STRUCTURE CHEMICAL STABILITY MULLITE FIBER	UNCLASSIFIED - UNLIMITED

19. Security Classif. (of this report)	20. Security Classif. (of this page)	21.
UNCLASSIFIED	UNCLASSIFIED	

FOREWORD

This report covers work performed under contract NAS 3-16764 for the period 1 July 72 through 31 August 1973. The work was administered by the NASA-Lewis Research Center with Mr. John P. Merutka as Project Manager.

Research efforts were performed under the direction of Mr. W. G. Long. Dr. A. V. Illyn, Technical Director of the Refractories Division, served as project director for this contract. Mr. H. L. Miller was responsible for the manufacture of fine diameter mullite fiber.

ABSTRACT

This report contains the results of a research program to develop and evaluate mullite fiber with a mean diameter under 2 microns. The 2-micron fiber is produced by a blowing process at room temperature from a low-viscosity (10-25 poise) solution. The blown fiber was evaluated for dimensional stability in thermal cycling to 1371C and was equivalent to the 5-micron spun B&W mullite fiber. An additive study was conducted to evaluate substitutes for the boron. Three levels of chromium, lithium fluoride, and magnesium were added to the standard composition in place of boron and the fiber produced was evaluated for chemical and dimensional stability in thermal cycling to 1371C. The magnesium was the most chemically stable, but the chromium additive imparted the best dimensional stability.

CONTENTS

List of Tables

Tables (Cont'd)

List of Figures

Figures (Cont'd)

1. SUMMARY

A new blowing process was developed to reduce the average mullite fiber diameter from an average of 5 microns as manufactured by the commercial spinning process to below 3 microns to be comparable in diameter to available silica fiber. This development allows the maximum utilization of the approximately 100°C operating temperature advantage which mullite possesses over silica. The thermal conductivity of a fibrous product is a direct function of the fiber diameter.

Mullite fiber was produced with a total of fifty-four individual combinations of blowing process variables. Each fiber sample was examined for fiber diameter distribution. The process variables which produced the finest diameter fiber in the first forty-one combinations were identified and thirteen additional process variable combinations were selected for optimization of the blowing process. These thirteen fiber samples were examined for fiber diameter distribution and shot content. The average fiber diameter for seven of these thirteen fiber samples was two microns or less. This represented a significant reduction in fiber diameter from the commercial B&W mullite fiber, which had an average fiber diameter of approximately five microns.

Two pound batches of mullite fiber were manufactured with the optimum process variables and subjected to thermal cycling to 1259C and 1371C. Results of this thermal exposure indicated that the fine diameter fiber produced by the blowing process was equivalent in thermal stability to the five micron mullite fiber produced by centrifugal spinning. Table 1 compares the properties of the blown fiber prepared in this program with the B&W mullite fiber previously manufactured by centrifugal spinning.

Table 1. Comparison of Blown and Spun Mullite Fiber Properties

	Spun mullite	Blown mullite
Mean Fiber Dia.,μ	4.7 - 5.0	1.7 - 2.0
Shot Content	9 - 38	38 - 53
Linear Shrinkage, % After 25 Thermal Cycles	< .5 (1200C)(1) <1.0 (1325C)	< .5 (1259)(2) <1.0 (1371C)
Chemistry, Mole %	67.7 Al_2O_3 25.5 SiO_2 5.8 B_2O_3 1.0 P_2O_5	Same as spun

(1) Measured on bulk fiber after cycling to 1200C and 1325C (reference 1).
(2) Measured on pads from chopped fiber after cycling to 1259C and 1371C.

An additive study was conducted to determine if a satisfactory substitute could be made for the boron content in the standard B&W mullite composition. Boron has a relatively high vapor pressure at temperatures above 1200C and tends to vaporize. The result is a progressive diminution of the boron content. Chromium, magnesium, and lithium were each added at three different concentration levels as a boron substitute. The chromium additive was the most stable and appeared to offer excellent thermal stability at the five weight percent additive level.

A second consideration in the additive study was to determine the effect of the three additives in retarding grain growth at temperature in the mullite fiber. Based on scanning electron microscope examination of the fiber surface and cross-section, no significant change in the degree of grain growth was effected.

The blowing process was scaled up from a production rate of .22 lb/hr to 10 lb/hr. Fiber was produced at 10 lb/hr, although the quality was poor. Additional development efforts are required to define the proper combination of blowing process parameters to produce satisfactory mullite fiber at 10 lb/hr.

The results of this project indicate that mullite fiber can be produced in a finer diameter by the blowing process than was previously possible by centrifugal spinning. The mullite fiber produced in the blowing process has an equivalent level of thermal stability. The blowing process can be scaled up, which should allow the production of fine diameter mullite fiber at lower costs. Chromium is a more thermally stable additive than boron at temperatures to 1371C. No change in the grain growth characteristics in mullite fiber was effected in the additive study.

2. INTRODUCTION

Previous development work has demonstrated the excellent thermal stability of B&W mullite fiber produced by a centrifugal spinning technique with an average fiber diameter of approximately five microns[1].

In tests of several fiber systems for utilization on the Thermal Protection System of the Space Shuttle, it was shown that the thermal conductivity was a direct function of fiber diameter[2]. With the excellent dimensional stability of the mullite fiber at Space Shuttle service temperatures, the feasibility of producing finer diameter mullite fibers was examined.

Prior to the initiation of this program, a laboratory-scale blowing process was assembled in the Research & Development Division of Babcock & Wilcox and fiber samples were produced. The mean diameter of these fibers was significantly lower (<3 microns) than previously produced by centrifugal spinning. This work formed the basis for the present contract.

The program is divided into two technical tasks and one reporting task to accomplish the above objectives. Task I involves a parametric study of several variables in the B&W Blowing Process, followed by a complete characterization of the 10 best variable combinations. The goals of Task I are to produce a mullite fiber with an average fiber diameter less than 3 microns, with 95 percent of a 100 fiber sample to be 6 microns or less in diameter. The shot content of this fiber should be no greater than is now present in the commercial B&W spun mullite fiber.

The standard B&W mullite composition which was utilized throughout Task I is as follows:

Oxide Constituent	Mole %
Al_2O_3	67.7
SiO_2	25.5
B_2O_3	5.8
P_2O_5	1.0

The Al_2O_3 and SiO_2 constituents will be held constant in Task II, with additive substitutes for the B_2O_3 and P_2O_5.

Task II involves a study of additives to the standard B&W mullite composition. The goals of Task II are to determine a mineralizer additive which promotes the low temperature formation of mullite and is less volatile than the B_2O_3. A further goal of Task II is to determine a suitable grain growth inhibiting additive to reduce the amount of grain growth experienced in standard mullite fibers at 1371C (2500F).

3. EXPERIMENTAL PROCEDURE - TASK I

3.1 Fiber Manufacture

All the mullite fiber evaluated in this program was manufactured by the B&W Blowing Process. A schematic of the equipment is given in Figure 1. The solution is fed through a narrow orifice into a nozzle where compressed air causes fiberization. The fiber is then fed through a duct into a collection bin.

The fiber is then fired to 1065C, converting the glassy material to polycrystalline mullite.

The variables in the blowing process were solution viscosity, air pressure, production rate, nozzle setting, and relative humidity. The ambient temperature was maintained at 28-30C. A parametric study of these variables was initiated to identify the combination which would produce the finest diameter mullite fiber.

3.2 Fiber Diameter

Initial determinations of fiber diameter were made at 450X using an optical microscope with a Vickers split image eyepiece. This technique had proven quite accurate and reproducible in previous development programs on mullite fiber. However, the fiber produced by the blowing process is significantly smaller in diameter, and the measurements taken were approaching the limits of resolution of an optical microscope ($\sim$1-2 microns).

The scanning electron microscope was utilized for all measurements of fiber diameters, following the failure with the optical system. A representative sample of fibers was taken from the fiber batch and examined at 600X.

Photographs were made of at least four areas from each fiber sample. These photographs were then enlarged to 3600X, and fiber diameters were measured from each photograph. From these measurements, the fiber diameter distribution and the mean diameter was determined.

3.3 Shot Content

Shot is defined as the unfiberized portion of the fiber product and is common to most refractory fibers. The shot content was determined by a water elutriation method using the apparatus shown in Figure 2.

Figure 1. Experimental Mullite Fiber Blowing Process

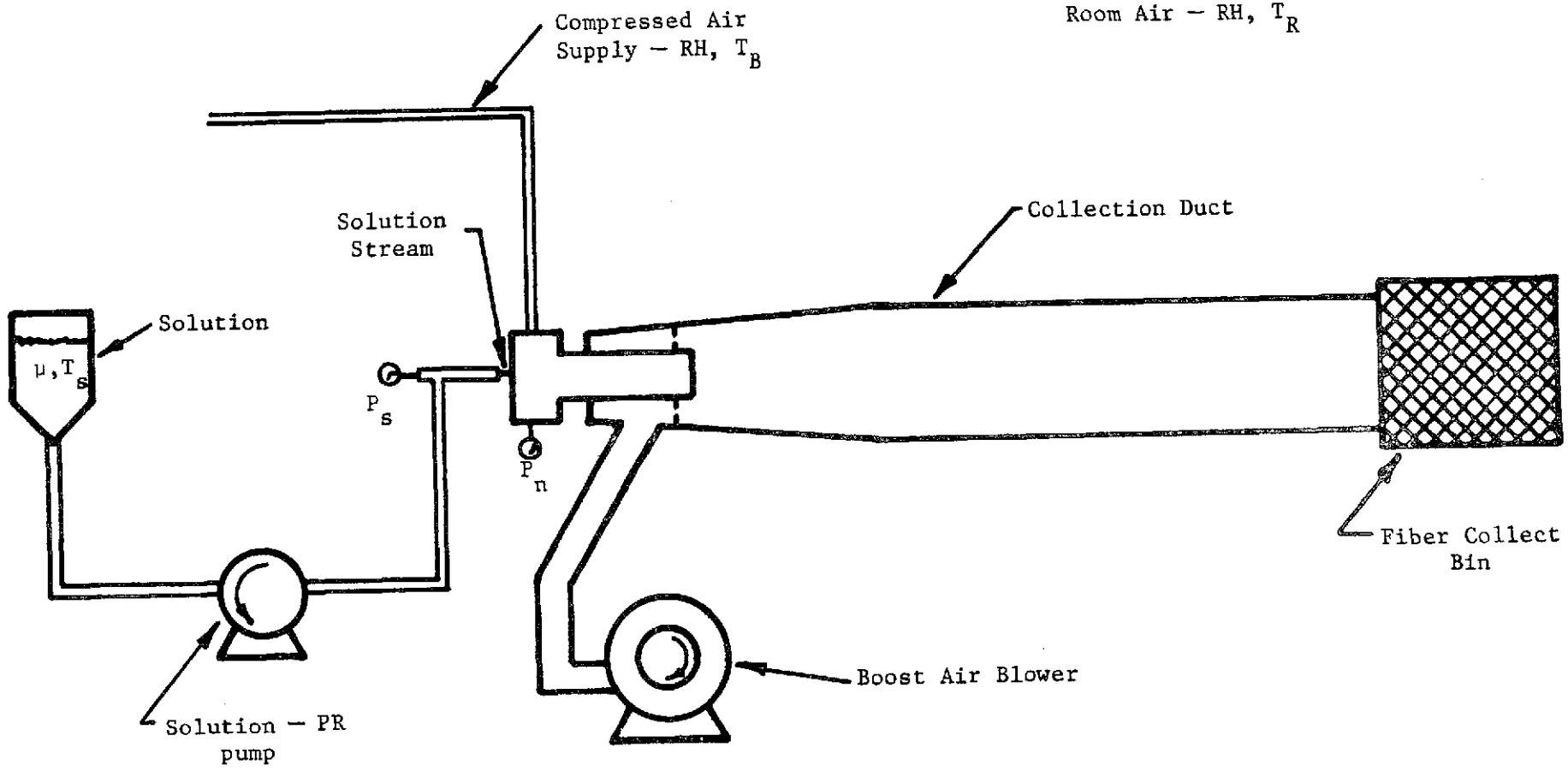

Independent System Variables

1. Solution viscosity, μ
2. Solution temp, T_S
3. Fiber production rate, PR
4. Blowing nozzle air pressure, P_n
5. Blowing nozzle setting, TO
6. Room air relative humidity, RH
7. Room air temperature, T_R
8. Blowing air relative humidity, RH
9. Blowing air temperature, T_B

Figure 2. Apparatus Used in Fiber-Shot Separation

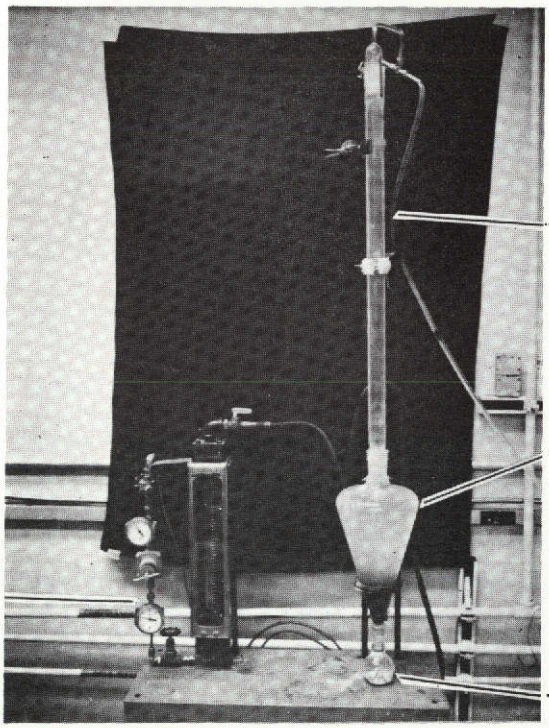

This page is reproduced at the back of the report by a different reproduction method to provide better detail.

The first step is the crushing of a 20 gram sample. This crushed sample is then placed in the inverted Erlenmeyer flask section. Water flow is then introduced at a predetermined rate, and the fiber is carried off through the vertical column along with the discharge water. The shot remains at the lower end of the Erlenmeyer flask and settles into the receptacle as the water flow is terminated. Microscopic examination of both the collected fiber fraction and the shot residue confirmed that this technique is highly efficient in separating shot from fiber.

3.4 X-Ray Diffraction Analysis

Diffraction patterns were generated using motor driven diffractometer synchronized with a recorder. The mullite fibers were ground in an agate mortar to pass a 100 mesh screen and then packed into an aluminum holder. Copper radiation with a nickel filter was used and the scanning rate was 2 degrees per minute. Crystalline components were identified using the ASTM powder diffraction index cards as a reference.

3.5 Surface Morphology

The surface condition of the fibers were examined using the scanning electron microscope (SEM) and the transmission electron microscope (TEM). Fiber samples were prepared for SEM examination by vapor plating a thin coating of gold or palladium. Bundles of fiber were encapsulated with epoxy prior to examination by the TEM. The fiber bundle was then fractured, and the exposed fiber in the fracture surface was replicated. The replicas were then shadowed at 30 degrees with palladium followed by carbon deposition at 90 degrees.

3.6 Fiber Pad Preparation

Fiber pads were prepared with and without binder for exposure to thermal cycling. The fiber was dispersed by forming a water slurry and agitating in a Waring blender for approximately 30 seconds. For those pads containing binder, a measured amount of colloidal silica was introduced in the slurry prior to blending. The pads made with a silica binder contained 10 weight percent silica.

The pads were formed in a filter press with a 2 inch diameter cavity. The 2 inch diameter by approximately 1 inch high pads formed were dried overnight. The dried pads, with and without binder, were then ready for cyclic elevated temperature exposure. Measurements of the diameter and height of each pad was recorded prior to thermal exposure to calculate thermal shrinkage.

3.7 Thermal Cycling

The 2 inch diameter fiber pads were subjected to 25 thermal cycles from room temperature to 1259C and to 1371C. A separate group of fiber pads was used for each temperature. A glo-bar fired furnace was maintained at the control temperature, 1259C and 1371C, and the fiber pads were introduced directly into the hot zone of the furnace and held at temperature for one hour. After one hour the pads were removed and allowed to cool to room temperature. This procedure was followed 25 times at 1259C on one group of fiber pads and again at 1371C on another group of fiber pads. This test subjected the fiber to thermal shock and to the extreme temperatures anticipated on the Space Shuttle vehicle.

3.8 Blowing Process Scale-Up

Tests were performed to evaluate the feasibility of scaling up the B&W blowing process from 0.22 to 10.0 lb/hr.

A schematic of the blowing system for the experimental mullite fiber as modified for the 10 lb/hr production is shown in Figure 3. The mullite solution is fed to a gear pump by gravity or by using a slightly pressurized (20-30 psig) solution vessel. The flow of solution is controlled by controlling the speed (rpm) of the gear pump, which has a capacity of 2.92 cc/revolution. The solution is pumped to a feed nozzle. Five types of solution feed nozzles were used during the testing. Three of the nozzles are single-orifice types, and two are multiple (six and nine) solution orifice types. Figure 4 shows sketches of the feed nozzles used for the testing.

The solution stream (or streams) from the solution feed nozzle enters the blowing nozzle. Two sizes of blowing nozzles were used during the testing. The nozzles are identical in configuration and only differ in size.

The solution is fiberized in the blowing nozzle, and the fibers travel down the collection duct to the collection belt. The fibers are then partially dried by the drying lamps above the collection belt and enter the tunnel kiln for final firing for about 15 minutes at 1065C.

Figure 3. Improved Continuous Blowing System

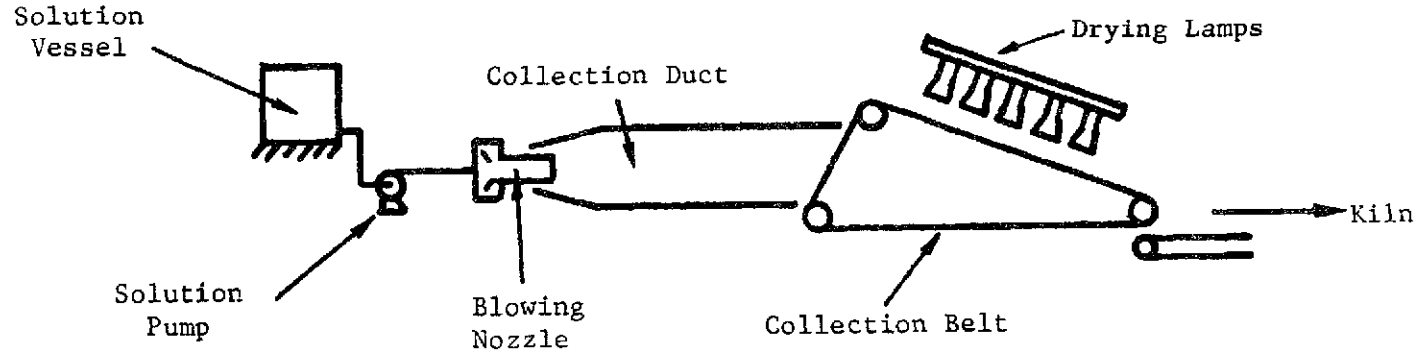

Figure 4. Solution Feed Nozzles

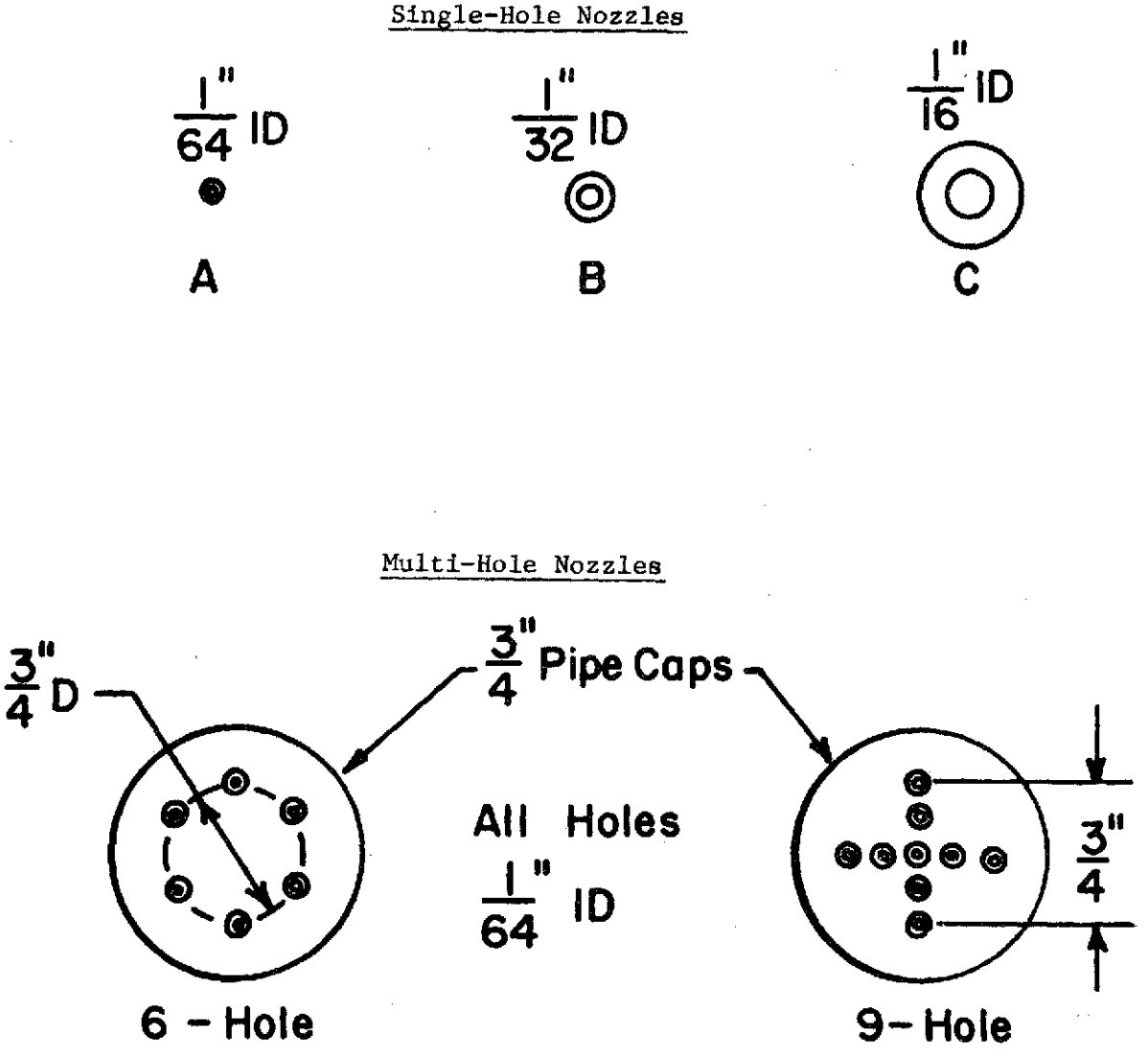

4. RESULTS AND DISCUSSION - TASK I

4.1 Blowing Process Parametric Study

A parametric study of the variables in the B&W blowing process was conducted to identify the combination of process variables which would produce the finest diameter mullite fiber. The blowing process involves the feeding of a room ambient temperature solution into a stream of compressed air, causing shearing of the solution droplets and thereby fiberizing the material.

The variables studied were solution viscosity, air pressure, production rate, nozzle setting, and room relative humidity. The fiberization room temperature was maintained at approximately 28-30C throughout this project. The first 18 combinations were grouped into test Series A. In this series, production rate was held constant at 100 grams/hour and the relative humidity in the fiberization room was maintained constant at 30 percent. The solution viscosity, air pressure, and nozzle setting were varied as shown in Table 2.

Fiber produced in each of these 18 combinations was examined with the optical microscope at 450X with 100 diameters read and the average fiber diameter calculated. This same procedure was followed for Series B and C. The absence of very fine (<1 micron) fiber was noted in the results of the optical microscope examination. At 1 micron, the limits of resolution of an optical system are approached, and we were unable to distinguish between 1 and 2 micron fiber diameters. The fiber diameters produced in test Series A, B, and C were re-examined and judged as to the lowest concentration of large diameter (>4 micron) fibers. The lower numbered runs in each test series tended to produce finer diameter fibers.

In Series A, runs A1, A2 and A3 produced finer diameter fiber than the higher numbered runs in the A Series. In Series B, whose process variables are given in Table 3, the finest diameters were produced in B1 through B4. These four runs were all made at 10 poise.

The process variables examined in test Series C are shown in Table 4.

Table 2. Parametric Study — Fiber Produced in Test Series A

Run	Viscosity (μ) poise	Production rate (PR), g/h	Air pressure (P_N), psig	Nozzle setting (TO), no. turns	Relative humidity, %
A1	10	100	22	1/2	30
A2	10	100	27	1/2	30
A3	10	100	32	1/2	30
A4	10	100	40	1/4	30
A5	10	100	50	1/4	30
A6	10	100	60	1/4	30
A7	25	100	22	1/2	30
A8	25	100	27	1/2	30
A9	25	100	32	1/2	30
A10	25	100	40	1/4	30
A11	25	100	50	1/4	30
A12	25	100	60	1/4	30
A13	50	100	22	1/2	30
A14	50	100	27	1/2	30
A15	50	100	32	1/2	30
A16	50	100	40	1/4	30
A17	50	100	50	1/4	30
A18	50	100	60	1/4	30

Table 3. Parametric Study — Fiber Produced in Test Series B

Run	Viscosity (μ) poise	Production rate (PR), g/h	Air pressure (P_N), psig	Nozzle setting (TO), no. turns	Relative humidity, %
B1	10	200	32	1/2	30
B2	10	300	32	1/2	30
B3	10	200	60	1/4	30
B4	10	300	60	1/4	30
B5	25	200	32	1/2	30
B6	25	300	32	1/2	30
B7	25	200	60	1/4	30
B8	25	300	60	1/4	30
B9	50	200	32	1/2	30
B10	50	300	32	1/2	30
B11	50	200	60	1/4	30
B12	50	300	60	1/4	30

Table 4. Parametric Study — Fiber Produced in Test Series C

Run	Viscosity (μ) poise	Production rate (PR), g/h	Air pressure (P_N), psig	Nozzle setting (TO), no. turns	Relative humidity %
C1	10	100	32	1/2	10
C2	10	100	32	1/2	30
C3	10	100	32	1/2	40
C4	10	100	32	1/2	60
C5	25	100	32	1/2	10
C6	25	100	32	1/2	30
C7	25	100	32	1/2	40
C8	25	100	32	1/2	60
C9	50	100	32	1/2	10
C10	50	100	32	1/2	40
C11	50	100	32	1/2	60

In test Series C, fiber was produced and collected for all 11 runs. The fiber in runs C2, C3, C4, C5, C8, C9, and C11 was of very poor quality. At the high humidity conditions of runs C2, C3, C4, C8, and C11, the solution tended to atomize rather than fiberize. Shearing of the droplets into fibers was minimal. This condition is apparently related to the effect of higher humidity on the surface tension of the solution droplets.

Since the optical microscope did not completely define the fiber diameter distribution, the scanning electron microscope was employed to characterize the fiber distribution in those runs in the A, B, and C Series which showed the lowest concentration of large diameter fibers. The fiber specimens which were selected are shown in Table 5. The values indicate that 60–70 percent of the fiber produced for most of these runs is finer than 2 microns, assuring that the mean diameter would be below 3 microns.

Table 5. Fiber Diameter Measurements

	DIAMETER, MICRONS				
Run No.	<1	1<2	2<3	3<4	>4
A1	22	42	20	15	
A2	30	41	19	8	
A3	30	35	22	11	3
B1	51	20	20	5	3
B2	58	25	5	5	4
B3	29	29	32	5	3
B4	40	27	21	8	3
C1	30	25	25	9	9
C6	30	20	20	10	20
C7	28	31	25	14	

Based upon the results produced in Test Series A through C, it appeared that the lower viscosity ranges produced the finest diameter fiber. Therefore, a range of 10-25 poise was selected for the final series. The optimum nozzle setting had been established at 1/2 turn. The air pressure to the nozzle was optimized at 32 psig in Test Series A through C for the 10 poise viscosity solution. For the 25 poise solution, 22 psig appeared to produce the finest fiber. For the DE Series, the production rate was varied between 100 and 300 grams per hour. The relative humidity was maintained between 14 and 27 percent. At higher values of relative humidity, 30 percent and above, the fiber tended to gel together in the duct and in the collection bin. The complete set of combinations of process variables for the final Series is shown in Table 6.

Table 6. DE Series Results

Run	Solution viscosity, poise	Nozzle setting, no. turns	Nozzle air supply press., psig	Fiber prod. rate, g/h	Relative humidity, %	Shot content %	Average* fiber diameter, μ
DE1	10	1/2	32	300	14	48	2.0
DE2	10	1/2	32	300	24	50	1.7
DE3	10	1/2	32	200	14	44	1.7
DE4	10	1/2	32	150	15	46	1.8
DE5	10	1/2	32	100	14	35	1.7
DE6	17	1/2	32	300	26	53	2.0
DE7	17	1/2	32	200	20	47	1.9
DE8	17	1/2	32	100	20	42	2.2
DE9	17	1/2	32	100	12	37	2.2
DE10	17	1/2	32	200	16	39	2.1
DE11	25	1/2	22	300	27	46	2.6
DE12	25	1/2	22	200	21	41	2.1
DE13	25	1/2	22	100	25	41	2.2

* Based upon 100 fiber measurements.

The shot content was measured for each individual run in the DE Series. As shown in Table 6, the shot contents ranged from 35 to 53 weight percent of the bulk fiber products. The lower shot contents appear to be produced at the lowest production rate and the lower values of relative humidity with the solution viscosity held constant. Thus, DE5 has the lowest shot content of any run at 10 poise viscosity. At the higher production rate, 300 grams/hour in DE1 with all other variables identical to DE5, the shot content was increased from 35 to 48 weight percent. Shot content tends to increase with production rate for all of the viscosities examined in the DE Series.

The shot content of spun mullite fiber ranges from a low of 9 percent to a high of 38 percent, based upon ten spun fiber samples examined by the water elutriation method.

The fiber diameters for all runs in the DE Series proved to satisfy the goals of this project. The average diameter of the fiber in individual runs ranged from 1.7 microns in runs DE2, DE3 and DE5 to 2.6 in DE11. In general, the lower averages are produced in those fiber samples where no large diameter fibers are produced. Consider DE2 and DE9 fiber diameters. Tables 7 and 8 show the fiber diameter distribution in these two fiber samples. The cumulative distribution shows the percent of individual fiber diameters less than the value in the left column of each table. For instance, in the DE2 fiber, 91 percent of the diameters measured were less than 3 microns. In the DE9 fiber, 85 percent of the fiber diameters were less than 3 microns. The significant difference between the DE2 and the DE9 average diameter values is in the fraction over 3 microns, particularly in the few fiber diameters over 5 microns in the DE9 fiber. Representative fibers from the DE2 and the DE9 runs are shown in Figures 5 and 6, respectively.

In general, the distribution of fiber diameters in the DE Series is similar for all 13 runs. This is a natural result of focusing in on the process parameters to a degree where further refinement produces no change in the fiber diameter distribution. Over 100 total combinations of process variables have been investigated during the course of research conducted by Babcock & Wilcox prior to this program, as well as the work described in this program.

X-ray diffraction patterns of the fiber samples in the DE Series show only gamma alumina and mullite present in crystalline form. No cristobalite was identified. The relative amounts of mullite and gamma alumina appear to vary, judging from the intensity of the x-ray diffraction peaks. These differences are a direct function of the firing temperature in the tunnel kiln. In the production of spun mullite fiber, x-ray diffraction patterns have typically exhibited varying amounts of gamma alumina present in the mullite fiber. The 1065C firing temperature for the mullite fiber is the minimum temperature at which the glassy fiber is converted to crystalline mullite. If the fiber is fired at a lower temperature due to variations in the furnace temperature, the conversion to mullite is less complete and significant amounts of gamma alumina remain.

Figures 7 through 9 illustrate the changes in the relative amounts of mullite and gamma-alumina as a function of time at temperature in a fiber specimen. The fiber in DE10 apparently was exposed to a temperature slightly under 1065C,

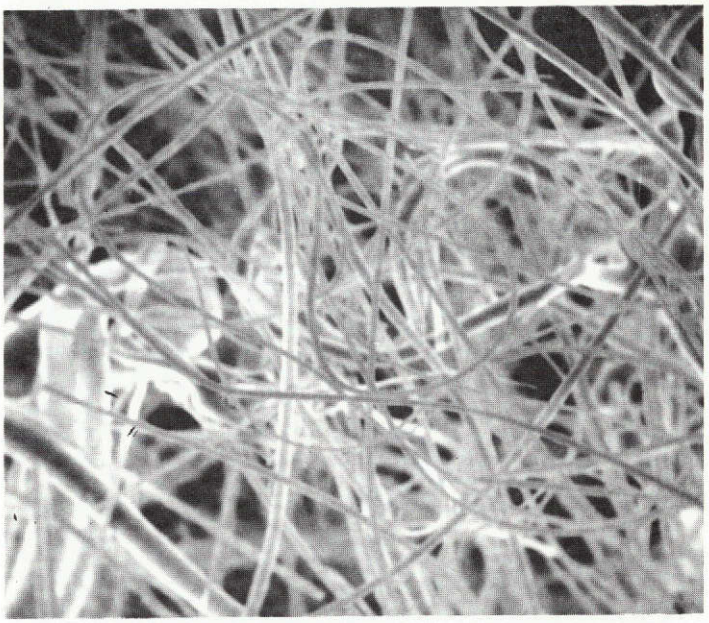

600X

Figure 6. DE-9 Fiber Examined by Scanning Electron Microscope

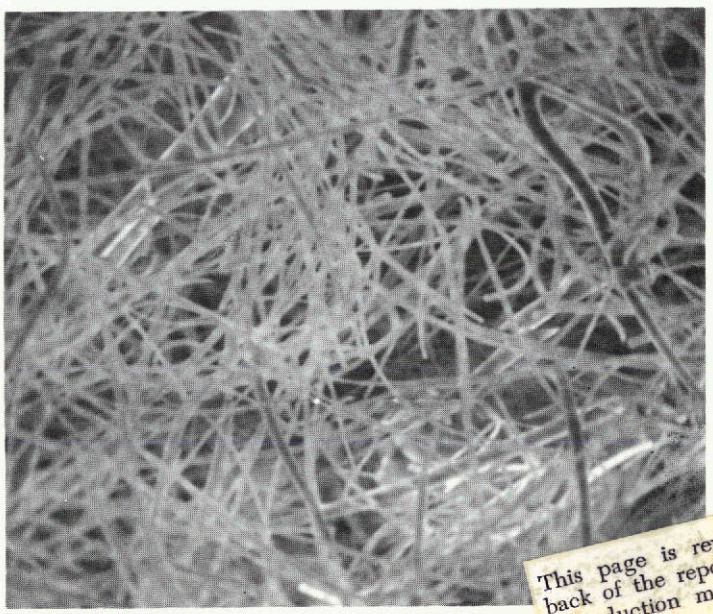

600X

Figure 5. DE-2 Fiber Examined by Scanning Electron Microscope

Figure 7. X-Ray Diffraction Pattern of DE-10 As-Manufactured Fiber

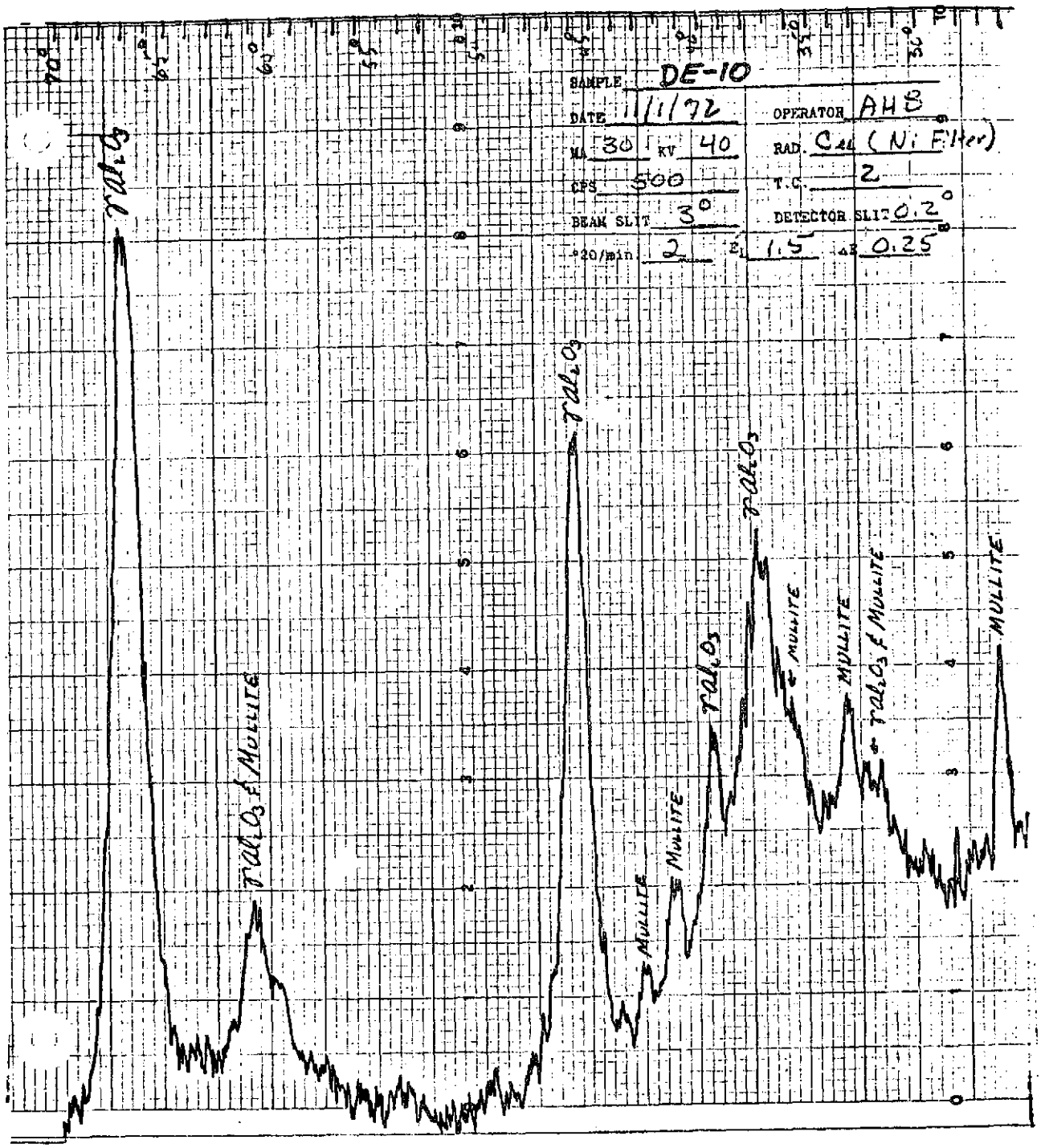

Figure 8. X-Ray Diffraction Pattern of DE-10 Fiber With 15 Minutes Additional Firing at 1065C

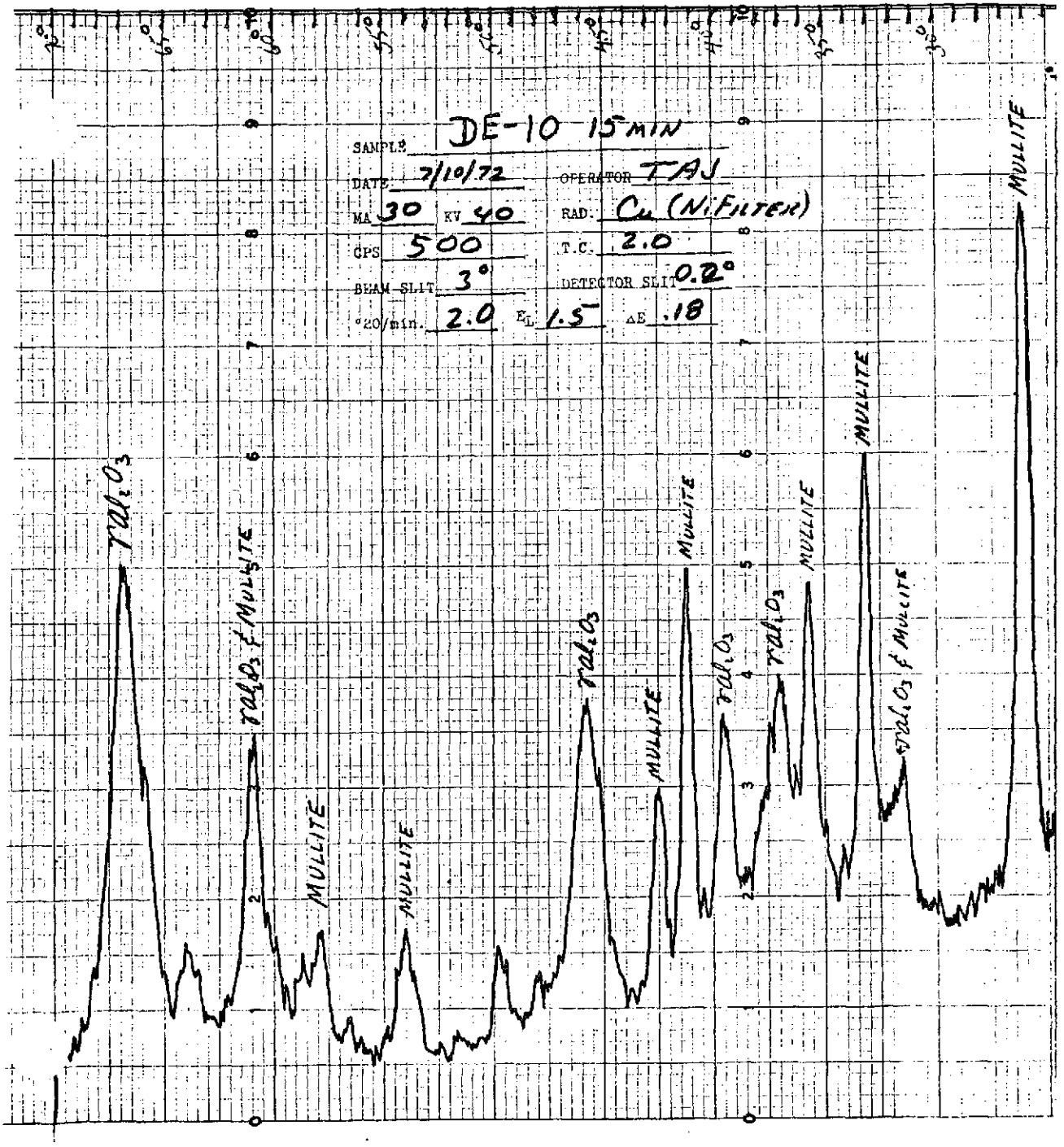

Figure 9. X-Ray Diffraction Pattern of DE-10 Fiber With 2 Hours Additional Firing at 1065C

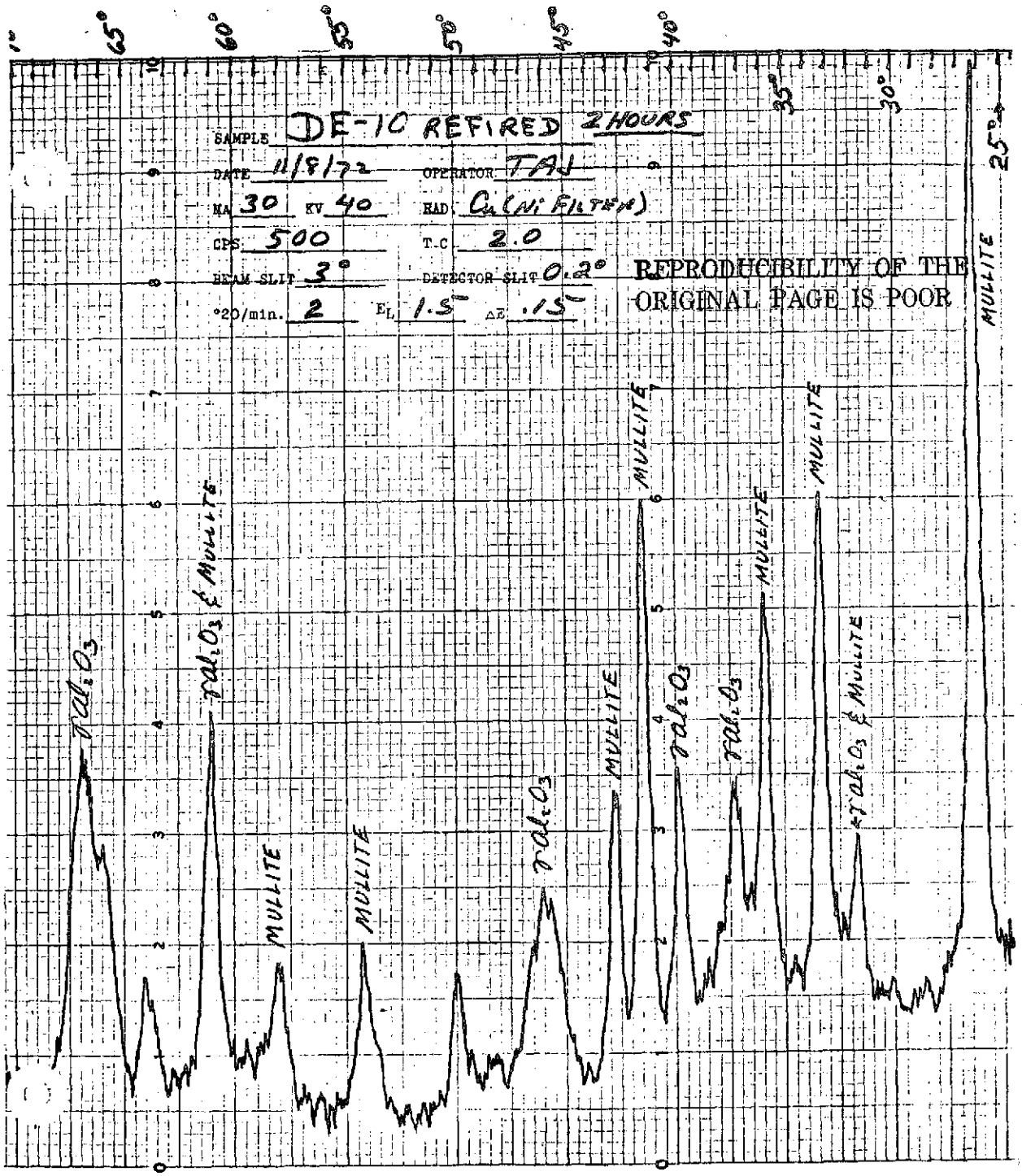

Table 7. DE-2 Diameter Distribution

(Arithmetic Mean = 1.7 μ)

Cumulative Distribution

Fiber Diameter Value, μ	Percent less than value
0.0	0
0.5	0
1.0	17
1.5	41
2.0	62
2.5	86
3.0	91
3.5	95
4.0	96
4.5	98
5.0	99
5.5	99

Ordered Array

0.5	1.0	1.5	2.0
0.6	1.5	1.5	2.0
0.7	1.1	1.5	2.0
0.7	1.2	1.5	2.2
0.8	1.2	1.5	2.2
0.8	1.2	1.5	2.2
0.8	1.2	1.7	2.4
0.8	1.2	1.8	2.4
0.8	1.2	1.8	2.4
0.8	1.2	1.8	2.4
0.8	1.2	1.8	2.4
0.8	1.2	1.8	2.5
0.8	1.2	2.0	2.5
0.9	1.2	2.0	2.5
0.9	1.2	2.0	2.5
0.9	1.4	2.0	2.5
0.9	1.5	2.0	3.0
1.0	1.5	2.0	3.0
1.0	1.5	2.0	3.0
1.0	1.5	2.0	3.2
1.0	1.5	2.0	3.5
1.0	1.5	2.0	4.0
1.0	1.5	2.0	4.0
1.0	1.5	2.0	4.5
1.0	1.5	2.0	5.5

NOTE: The ordered array is a display of the 100 fiber diameter measurements.

Table 8. DE-9 Diameter Distribution

(Arithmetic Mean = 2.2 μ)

Cumulative Distribution

Fiber Diameter Value, μ	Percent less than value
0.0	0
0.2	57
4.0	92
6.0	96
8.0	98
10.0	99
12.0	99
14.0	99
16.0	99
18.0	100

Ordered Array

0.8	1.4	1.8	2.2
0.8	1.4	1.8	2.2
0.9	1.4	1.8	2.2
0.9	1.5	1.8	2.2
1.0	1.5	1.8	2.2
1.0	1.5	1.8	2.5
1.0	1.5	1.9	2.7
1.0	1.5	2.0	2.8
1.0	1.5	2.0	2.8
1.0	1.5	2.0	2.8
1.1	1.5	2.0	3.0
1.1	1.7	2.0	3.0
1.2	1.7	2.0	3.0
1.2	1.8	2.0	3.0
1.2	1.8	2.0	3.2
1.2	1.8	2.0	3.2
1.2	1.8	2.0	3.8
1.2	1.8	2.0	4.0
1.2	1.8	2.0	4.0
1.2	1.8	2.0	5.0
1.3	1.8	2.0	5.0
1.4	1.8	2.0	6.0
1.4	1.8	2.0	6.0
1.4	1.8	2.2	8.0
1.4	1.8	2.2	17.0

producing the high gamma-alumina content. The same fiber, when refired at 1065C for 15 minutes, produced the pattern in Figure 8, which is typical of the other fiber specimens in this series. The mullite phase is predominant following this firing. Further exposure of 2 hours at 1065C produced the diffraction pattern shown in Figure 9, in which the mullite structure is more fully developed. (The complete series of 13 x-ray diffraction patterns is presented in the Appendix.)

The effect of underfiring on fiber quality is nebulous. The processing of fiber into tiles for the Space Shuttle evaluation involves a step in which the fiber tile is fired to 1259C. This firing converts the fiber to mullite. If the presence of gamma-alumina were determined to be detrimental, then an increase in firing the fiber would convert most of the gamma-alumina to mullite.

The surface morphology of the mullite fiber in the DE Series was examined at 3600X and at 30,000X on the scanning electron microscope. The fibers are extremely smooth with no significant morphology developed. Figures 10 and 11 show surface of typical fibers in the DE Series. These surface conditions are also typical of spun mullite fiber.

4.2 Blowing Process Scale-Up

Tests were performed to evaluate the feasibility of scaling up the B&W blowing process from 0.22 to 10 pounds of fiber per hour.

The original 100 grams per hour continuous production system resulting from the parametric study was initially set up. This system used solution feed nozzle A (Figure 4) and the mullite fiber blowing nozzle. The process variables used for this initial set up are as follows:

Solution viscosity (μ_S), poise	10
Air supply press (P_N), psig	32
Nozzle setting, turns open	1/2
Relative humidity (RH), %	25
System temperature (T_S), F	85
Production rate (FPR), lb/hr	.22

The solution feed rate was then gradually increased until the solution began to adhere to the inside diameter of the blowing nozzle. The limiting solution feed rate for this system is a fiber production rate of about 0.66 lb/hr. At this feed rate, solution adherence on the nozzle wall becomes prominent.

Figure 10. Surface of DE-2 As-Manufactured Fiber

30,000X

This page is reproduced at the back of the report by a different reproduction method to provide better detail.

Figure 11. Surface of DE-9 As-Manufactured Fiber

30,000X

It was believed that higher flows of mullite solution could be fiberized by increasing the air flow to the blowing nozzle. This was done by increasing the pressure of the air supply to the nozzle from 32 to 85 psig. As a result, at a nozzle setting of 1/2 turn open, the compressed air flow was increased from 160 lb/hr to about 425 lb/hr. Aspirated flow remained constant at 900 lb/hr.

Following these changes, it was found that the maximum allowable fiber production rate was still 0.66 lb/hr. Furthermore, when solution feed nozzles B and C (Figure 4) were substituted in place of feed nozzle A, the maximum allowable fiber production rate remained at 0.66 lb/hr. Also, as the chamber pressure was increased above 40 psig, the mullite solution tended to atomize rather than to fiberize.

Holding all other process variables constant, the viscosity of the solution was increased to 75 poise. This increased the maximum fiber production rate from 0.66 to 2.2 lb/hr. For this test run, the air supply pressure was 85 psig, and the nozzle setting was 1/2 turn open.

Again holding all process variables constant, a series of tests were run to determine the effect of the number of solution streams on the maximum allowable fiber production rate. From this series of tests, it was concluded that multiple-solution feed nozzle orifices allowed slightly higher rates of fiber production, and that a solution viscosity of 75 poise, a nozzle air supply pressure of 85 psig, and a setting of 1/2 turn open yield a satisfactory fiber.

At this point, it was obvious that higher solution viscosities would allow higher rates of fiber production; however, previous work had shown that higher viscosities also result in fibers of larger diameter. Since it was desired to minimize the diameter of fiber during this test program, a decision was made to install the larger blowing nozzle rather than to increase viscosity further in attempting to reach the goal of 10 lb/hr. The maximum compressed air flow available when using the larger nozzle was about 743 lb/hr. This flow was achieved with a supply pressure of 52 psig and a nozzle setting of 1 3/4 turns open.

Another system change made at this time was to pressurize the inlet to the gear pump to from 20 to 30 psig. At the higher flows of mullite solution, the gear pump tended to cavitate and to interrupt the solution stream. Pressurizing the inlet to the pump enables the inlet to remain flooded and prevents cavitation.

Using the larger nozzle at an air supply pressure of 52 psig and a nozzle setting of 1 3/4 turns, the goal of producing 10 lb/hr of fiber was reached.

Five production runs were made at fiber production rates of about 10 lb/hr. However, the mullite fiber produced at this rate was extremely short. Further work will be required on the process variables to optimize fiber at 10 lb/hr. The shot content for the five batches of fiber produced at 10 lb/hr was not significantly different from that produced at 0.22 lb/hr. The appearance of the fiber gives the illusion of a much higher shot content, probably due to the short fiber length. The shot content ranged from 42 to 53 wt %. In contrast, the shot content of the 2 pound batches produced for the thermal cycled pads ranged from 45 to 54 wt %. It is apparent that product quality can be optimized only through a systematic parametric study similar to the study that resulted in optimizing product quality at the 100 g/hr production rate. The scale-up study is summarized in Table 9.

Table 9. Scale-Up Study Summary

Solution viscosity, poise	Air supply pressure, psig	Nozzle setting, turns open	Production rate, lb/hr	No. solution nozzle orifices	Fiber quality
10	32	1/2	.66	1	Satisfactory
10	85	1/2	.66	1	Unsatisfactory-solution atomized
75	85	1/2	2.2	1	Satisfactory
75	85	1/2	3.4	6	Satisfactory
75	85	1/2	3.7	9	Satisfactory
75	52	1 3/4	10	9	Short fiber-typical shot content

During these production runs, it proved to be desirable to minimize relative humidity so that the fibers were as dry as possible before being collected on the fiber collection belt. However, previous work had shown that relative humidities below about 20% result in fiber of a brittle texture after firing; this condition was also apparent during the current testing.

Several system hardware changes were suggested following the testing. The velocity of the fiber should be reduced before collection to prevent the fiber's tending to fuse upon impact on the collection belt. The air velocity of the duct could be reduced by expanding the duct.

An attendant problem encountered at the higher production rates involved insufficient drying of the fibers before collection. This problem is probably

due to a high concentration of moisture in the air in the collection duct. To enable sufficient drying of fibers in the collection duct, additional drying air could be supplied to the duct, or the air in the collection duct could be heated.

In summary, it appears that hardware changes, along with a comprehensive parametric study similar to that for the production of fiber at 100 g/hr, will permit the production of mullite fiber at 10 lb/hr.

4.3 Thermal Exposure Evaluation

Based on the results of the DE series fiber evaluation, five of the best combinations of variables were selected to form series F. In this series, 2 pound batches of fiber were manufactured for thermal exposure evaluation.

The process variables selected for the five 2 pound batches are given in Table 10, together with the shot contents of F-1 through F-5. The range of shot content values indicates that the process variables produce very little difference in the five batches of mullite fiber.

Table 10. Process Variables and Shot Content for Two-Pound Batches

Run	Solution viscosity, poise	Nozzle setting, no. turns	Nozzle press., psig	Fiber prod. rate, g/h	Rel. humid., %	Room temp. F	Shot content, wt %
F1	10	1/2	32	100	25	85	45.2
F2	10	1/2	32	150	25	85	46.4
F3	10	1/2	32	200	25	85	47.4
F4	10	1/2	32	300	25	85	53.6
F5	10	1/2	32	300	15	115	50.2

In general, the fiber diameter distribution of all fiber groups in the DE and F series is very similar. The diameter distributions for fibers taken from groups F-1 and F-4 are given in Tables 11 and 12. The values in these tables indicate that the parameter changes have little effect on the distribution of fiber diameters.

The reduction in fiber diameter produced in this program compared to spun mullite is demonstrated by examining Figures 12 and 13. The F-4 series fiber distribution peaks at approximately 1.5μ, while the fiber produced by centrifugal spinning, shown in Figure 12, peaks at from 4 to 5μ. This reduction in fiber diameter should produce a significant increase in high-temperature insulating properties. At temperatures above approximately 800C, the primary modes of heat transfer in a fiber insulation system are radiation and gas conduction. For a given

Table 11. Run F-1 Fiber Size Data

(Average Diameter = 2.8 μ)

Cumulative Distribution

Fiber Diameter Value, μ	Percent less than value
0.5	0
1.0	1
1.5	14
2.0	30
2.5	45
3.0	59
3.5	71
4.0	79
4.5	89
5.0	96
5.5	96
6.0	97
6.5	98
7.0	99

Ordered Array

0.9	1.8	2.6	3.6
1.0	1.8	2.6	3.6
1.0	1.8	2.7	3.8
1.0	1.9	2.7	3.8
1.0	1.9	2.8	4.1
1.0	2.0	2.8	4.1
1.0	2.0	2.8	4.2
1.1	2.0	2.9	4.2
1.1	2.0	2.9	4.2
1.1	2.0	3.0	4.2
1.2	2.0	3.0	4.2
1.3	2.0	3.0	4.2
1.4	2.1	3.1	4.2
1.4	2.1	3.1	4.3
1.5	2.2	3.1	4.6
1.5	2.2	3.2	4.6
1.5	2.2	3.2	4.6
1.5	2.2	3.2	4.6
1.6	2.3	3.2	4.8
1.7	2.3	3.3	4.8
1.7	2.5	3.4	4.8
1.7	2.5	3.5	5.8
1.7	2.5	3.5	6.0
1.8	2.5	3.5	6.5
1.8	2.5	3.5	7.0

NOTE: The ordered array is a display of the 100 fiber diameter measurements.

Table 12. Run F-4 Fiber Size Data

(Average Diameter = 1.8 μ)

Cumulative Distribution

Fiber Diameter Value, μ	Percent less than value
0.0	0
0.5	0
1.0	12
1.5	35
2.0	70
2.5	85
3.0	90
3.5	91
4.0	94
4.5	97
5.0	100

Ordered Array

0.5	1.2	1.6	2.0
0.7	1.2	1.7	2.0
0.7	1.2	1.7	2.0
0.8	1.2	1.7	2.1
0.8	1.4	1.7	2.2
0.8	1.4	1.7	2.2
0.9	1.4	1.8	2.2
0.9	1.4	1.8	2.2
0.9	1.4	1.8	2.2
0.9	1.4	1.8	2.3
0.9	1.5	1.8	2.5
0.9	1.5	1.8	2.5
1.0	1.5	1.8	2.5
1.0	1.5	1.8	2.7
1.0	1.5	1.8	2.7
1.0	1.5	1.8	3.0
1.0	1.5	1.8	3.5
1.0	1.5	1.8	3.5
1.0	1.5	1.8	3.8
1.0	1.5	1.9	4.0
1.0	1.5	2.0	4.0
1.1	1.5	2.0	4.0
1.1	1.5	2.0	4.5
1.2	1.5	2.0	4.7
1.2	1.5	2.0	4.9

NOTE: The ordered array is a display of the 100 fiber diameter measurements.

Figure 12. Fiber Diameter Distribution in Mullite Fiber

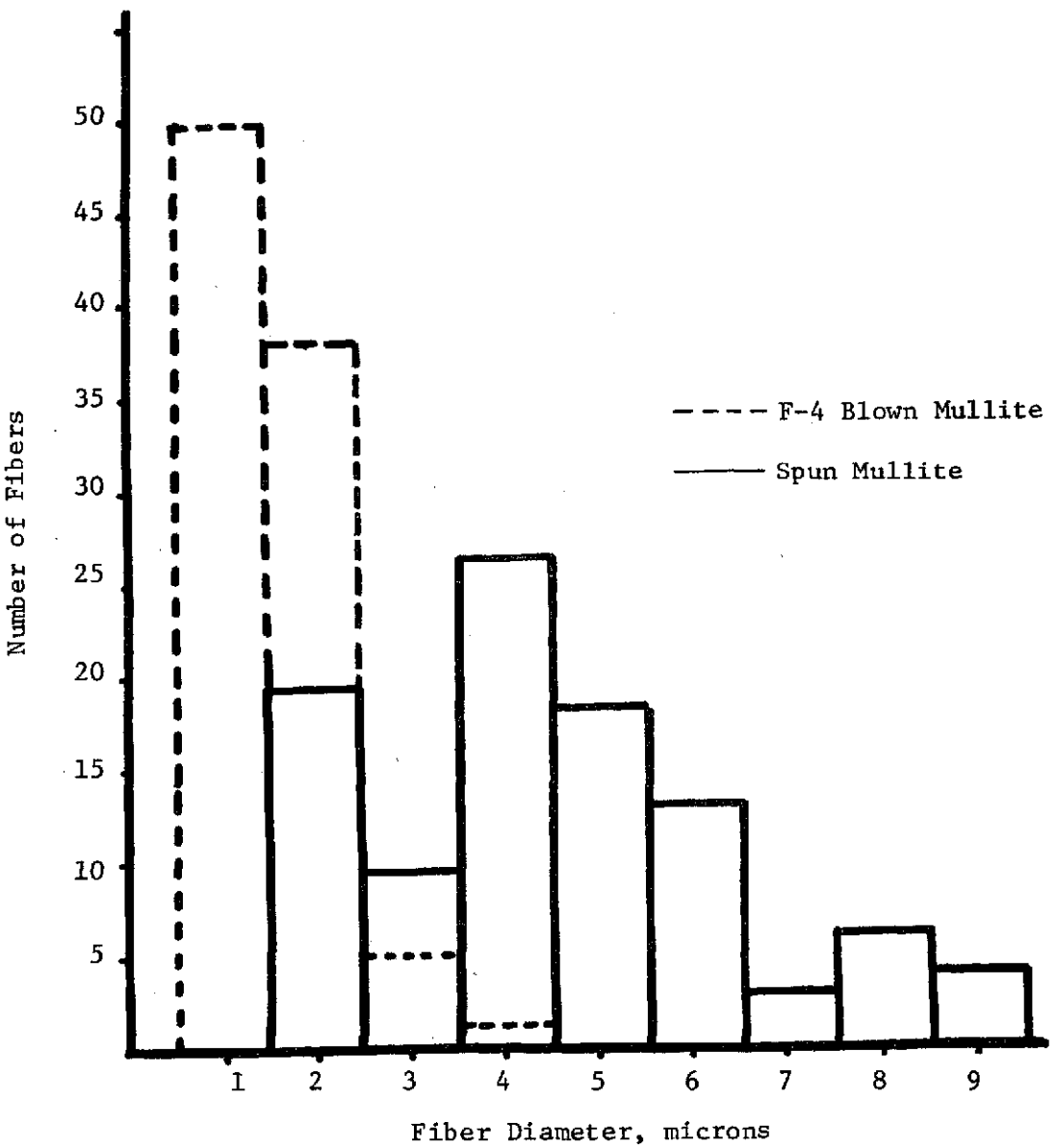

Figure 13. Fiber Diameter Distribution in Mullite Fiber From Run F-1

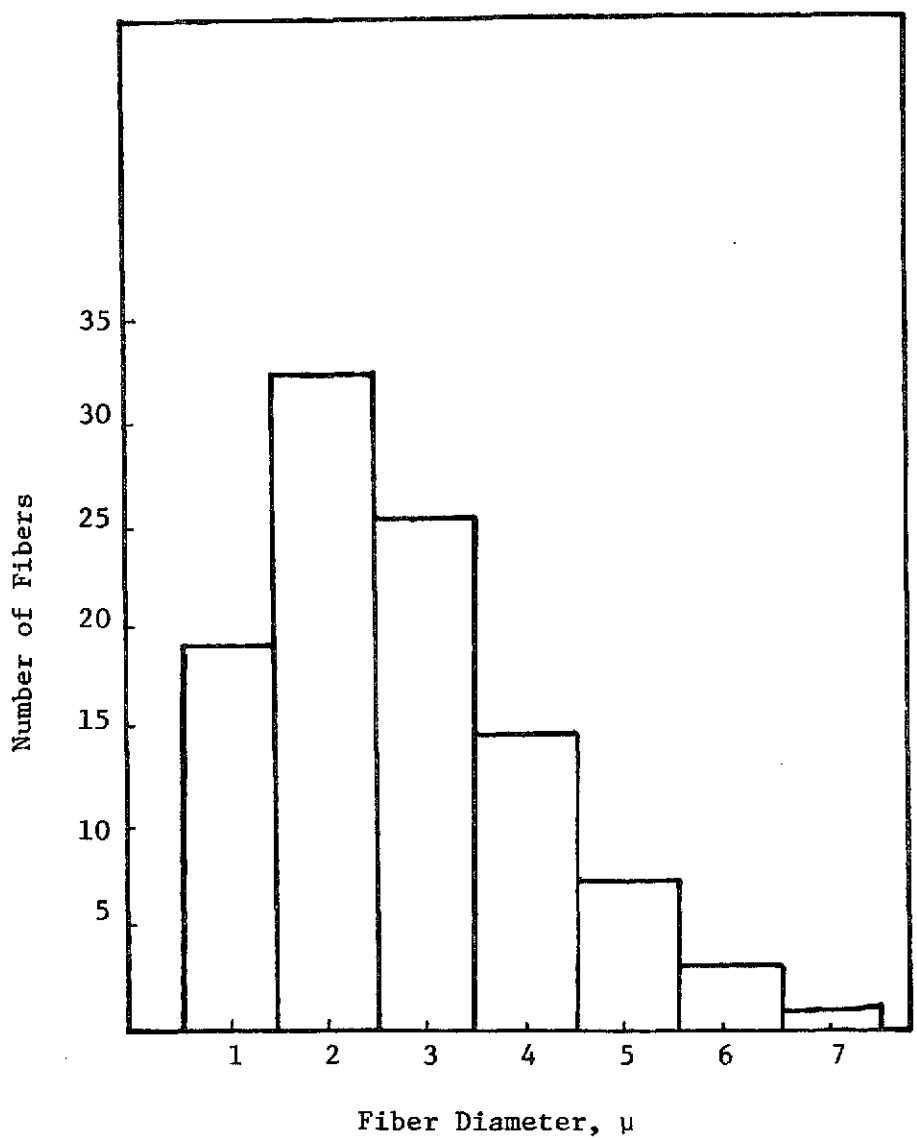

Figure 14. Pads Made From F-1 (left) and F-4 Fiber

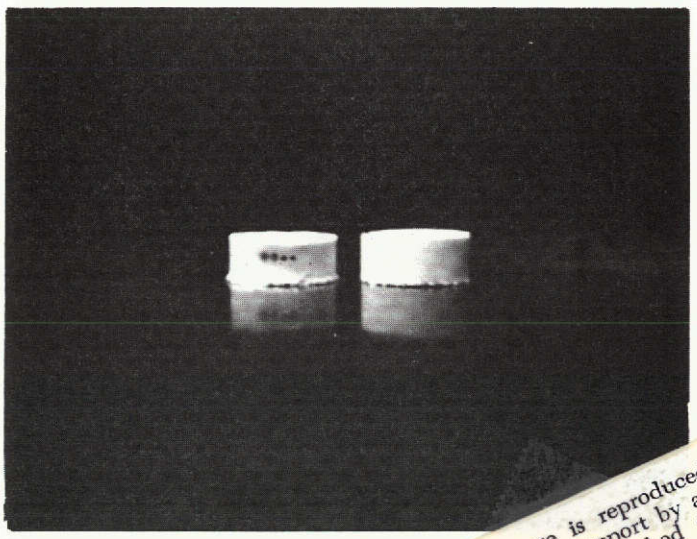

density of material, finer diameter fibers increase the interference to radiant energy flow and reduce the gas and conduction. This effect has been demonstrated in several fiber specimens of varying diameters in reference 2.

To evaluate the effects of thermal exposure on fine diameter mullite fiber, pads were prepared with and without colloidal silica binder. The pads, made in a 2 inch die by a filtration process, were dried overnight before cyclic elevated temperature exposure. Two typical pads are shown in Figure 14. Pads without binder delaminated and cracked during drying and continued to crack during the thermal cycle exposure. Most of the pads remained intact after the 25 thermal cycles.

The pads made with a binder contained 10 wt % colloidal silica, which was intimately mixed with the fiber before forming the pad. The pads were introduced into a furnace at 1259C held for 1 hour, removed from the furnace, and allowed to cool in air. This process was repeated 25 times. Following thermal cycling, the diameter and the height of each pad were measured. This procedure was repeated for the 1371C exposure.

Dimensional measurements taken before and after the 25 thermal cycles are given in Tables 13 and 14. After 1259C cycling, the shrinkage is less than 0.5% in the pads with silica binder. No significant difference between F1 and F4 fiber samples can be discerned. In specimens with colloidal silica binder, the average diametral shrinkage is less than 1% after the 1371C thermal cycling. The height shrinkage ranged from 0.41 to 1.90% for all fiber pads with binder.

The pads without binder experienced greater shrinkage. However, the delaminations in these pads were so severe that any conclusion on shrinkage may be meaningless. The effect may be due to mechanical shifting caused by handling and by thermal shock during the thermal exposure tests.

Fiber specimens from lots F1 and F4 were prepared by encapsulating fibers in an epoxy matrix, fracturing the composite formed, and then examining the exposed fiber surface.

The surface of an as-manufactured fiber from the F1 series is shown in Figure 15 as viewed by the scanning electron microscope. The smooth surface indicates no grain growth or roughening. Figure 16 shows an F4 fiber after exposure at 1259C. Some grain growth has been developed along with consequent surface roughening. Figure 17 shows the F1 fiber after exposure at 1371C. Although the surface appears to be extremely rough and the grains appear to have grown excessively, the average grain size is apparently less than 0.2 μ. This size is an approximation, considering that the fiber in Figure 17 is 2 μ in diameter.

Table 13. Dimensional Stability Following 1259C Thermal Cycles on Blown Mullite Fiber in F1 and F4 Production Lots

Sample	Initial diameter, in.	Final diameter, in.	Change, %	Initial height, in.	Final height, in.	Change, %
F1 #1 binder	2.037	2.071	+ 1.67	0.825	0.825	0.00
F1 #2 binder	2.047	2.054	+ 0.34	0.739	0.740	0.14
F1 #3 binder	2.015	2.025	+ 0.50	0.768	0.769	+ 0.13
F1 #4 binder	2.017	2.026	+ 0.50	0.833	0.833	0.00
F1 - no binder	2.03	2.04	+ 0.50	0.95	0.94	- 1.05
F4 #1 binder	2.037	2.044	+ 0.34	0.960	0.951	- 0.94
F4 #2 binder	2.032	2.038	+ 0.30	0.791	0.802	+ 1.39
F4 #3 binder	2.000	2.004	+ 0.20	0.906	0.904	- 0.22
F4 #4 binder	2.028	2.032	+ 0.20	0.918	0.914	- 0.44
F4 - no binder	2.06	2.06	0.00	1.38	1.32	- 4.35

Table 14. Dimensional Stability Following 1371 C Thermal Cycles on Blown Mullite Fiber in F1 and F4 Production Lots

Sample	Initial diameter, in.	Final diameter, in.	Change, %	Initial height, in.	Final height, in.	Change, %
F1 #1 binder	2.007	2.010	+ 0.15	1.028	0.016	- 1.17
F1 #2 binder	2.014	2.000	- 0.70	0.850	0.858	+ 0.94
F1 #3 binder	2.006	2.009	+ 0.15	0.706	0.693	- 1.84
F1 #4 binder	1.992	1.980	- 0.60	0.971	0.975	+ 0.41
F1 #1 no binder	2.04	2.01	- 1.47	1.25	1.19	- 4.80
F1 #2 no binder	2.05	2.01	- 1.99	0.94	0.91	- 3.19
F1 #3 no binder	2.12	2.05	- 3.30	1.15	1.14	- 0.87
F1 #4 no binder	2.04	1.99	- 2.45	1.17	1.13	- 3.42
F4 #1 binder	2.010	1.977	- 1.64	0.987	0.974	- 1.32
F4 #2 binder	2.036	2.024	- 0.59	1.039	1.029	- 0.96
F4 #3 binder	2.037	2.037	0.0	0.892	0.875	- 1.90
F4 #4 binder	2.014	2.009	- 0.25	0.992	0.982	- 1.01
F4 #1 no binder	1.99	1.95	- 2.01	1.27	1.24	- 2.36
F4 #2 no binder	2.05	---	---	1.30	---	---
F4 #3 no binder	2.02	1.93	- 4.45	1.24	1.19	- 4.03
F4 #4 no binder	2.00	1.93	- 3.50	1.27	1.23	- 3.15

Figure 15. Blown Mullite Fiber As-Manufactured (Lot F-1)

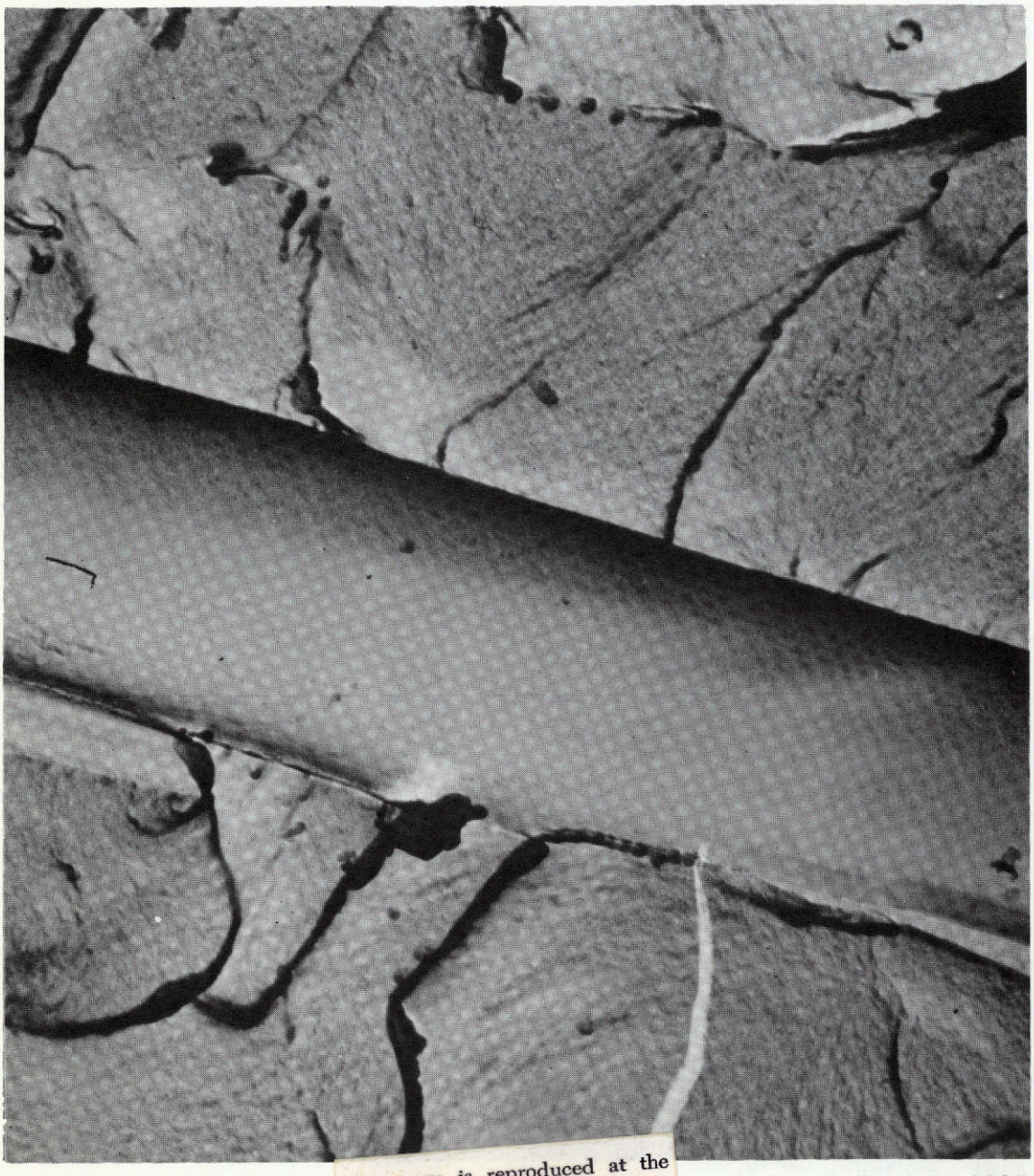

15,000X

This page is reproduced at the back of the report by a different reproduction method to provide better detail.

Figure 16. Blown Mullite Fiber Following 1259C Thermal Cycling (Run F-4)

30,000X

This page is reproduced at the back of the report by a different reproduction method to provide better detail.

Figure 17. Blown Mullite Fiber Following 1371C Exposure (Lot F-1)

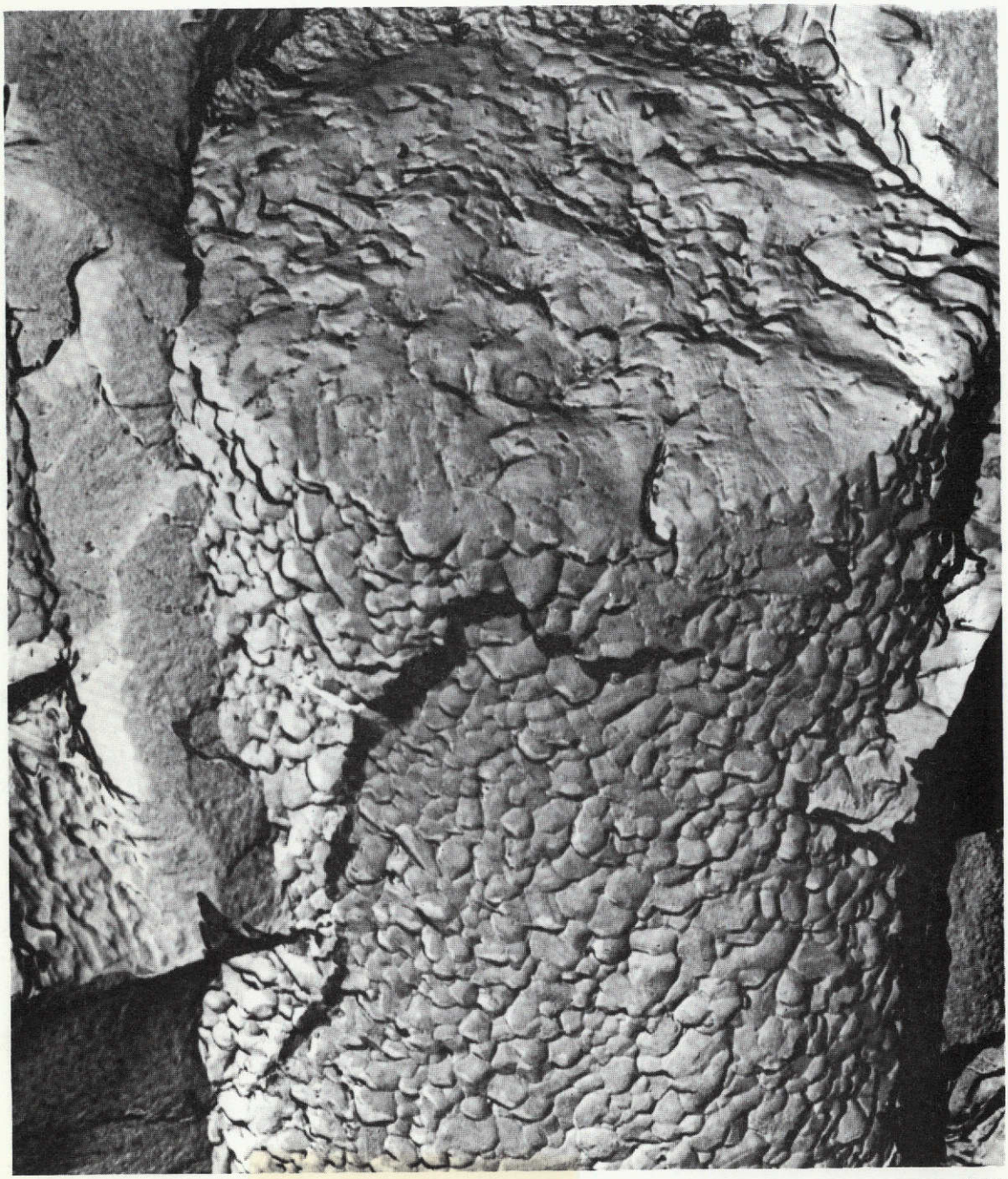

30,000X

Figure 18. Blown Mullite Fiber From F-4 Pad With Binder Following 1371C Exposure

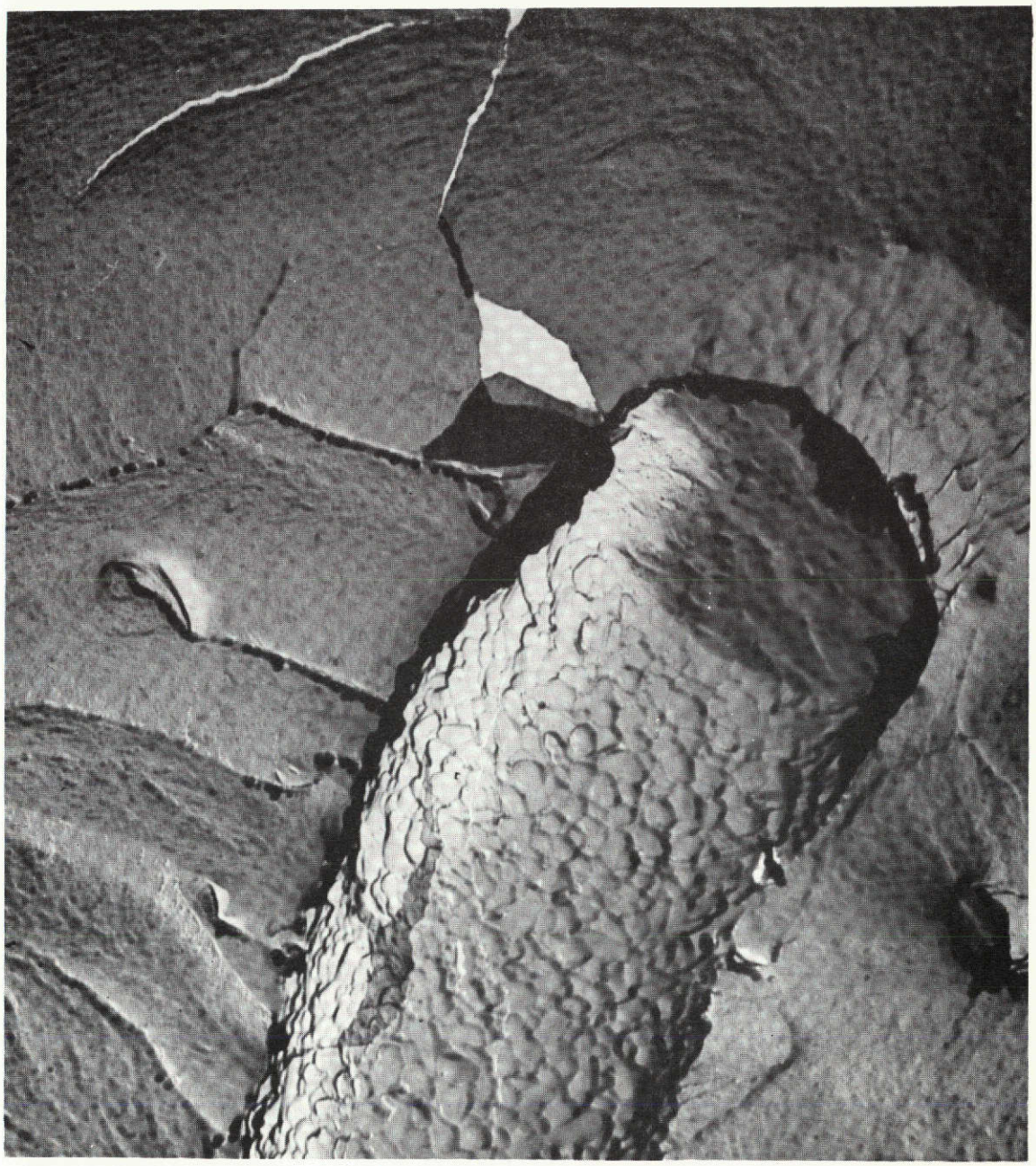

20,000X

This page is reproduced at the back of the report by a different reproduction method to provide better detail.

Ceramics with a grain size under 0.2 μ are normally considered to be fine grain.

Figure 18 shows an F4 fiber after exposure at 1371C. This fiber was taken from a pad containing binder. There is little difference in the grain size of the fiber between Figure 16 and Figure 18, which shows an F4 fiber without binder. The binder does not appear to influence the ultimate development of grain size.

The x-ray diffraction patterns for the thermally exposed blown mullite fiber from lot F1 are given in Figures 19 and 20. Figure 19 shows the diffraction pattern of the mullite fiber after the 1259C thermal cycling. Mullite is the only crystalline phase indicated in this pattern. Gamma-alumina or poorly defined alpha-alumina should also be present because of the excess of alumina in the mullite fiber composition. Figure 20 shows the mullite fiber after exposure at 1371C. The mullite crystalline phase is now accompanied by a minor amount of alpha-alumina. The presence of alpha-alumina at 1371C, which was absent at 1259C, may be related to the volatilization of the B_2O_3. Boron retards the formation of alpha-alumina, and the chemistry of the mullite fiber after 1259C shows only a slight decrease in boron concentration. After 1371C, the boron content has been reduced from an original 5.2% to 2.2%.

The relative changes in chemistry for the F1 mullite fiber as a function of thermal exposure are as follows:

	Chemical composition, wt %			
Thermal Exposure	Al_2O_3	SiO_2	B_2O_3	P_2O_5
As-manufactured	78.5	16.3	5.3	1.9
1259C (2300F)	78.8	16.6	3.1	1.7
1371C (2500F)	79.3	17.5	2.2	1.5

This quantitative analysis was performed by wet chemistry techniques. The results are similar to those for the chemical analyses made after thermal exposure of centrifugally spun mullite fiber.

SEM examination of the fiber pads was performed before and after thermal exposure to determine the general condition of the fiber and the consistency of the fiber pad. Figure 21 shows areas representative of F1 and F4 pads at the surface and at the center of the pad before thermal cycling.

Figure 19. X-Ray Diffraction Pattern of F-1 Fiber After 1259C Thermal Cycling

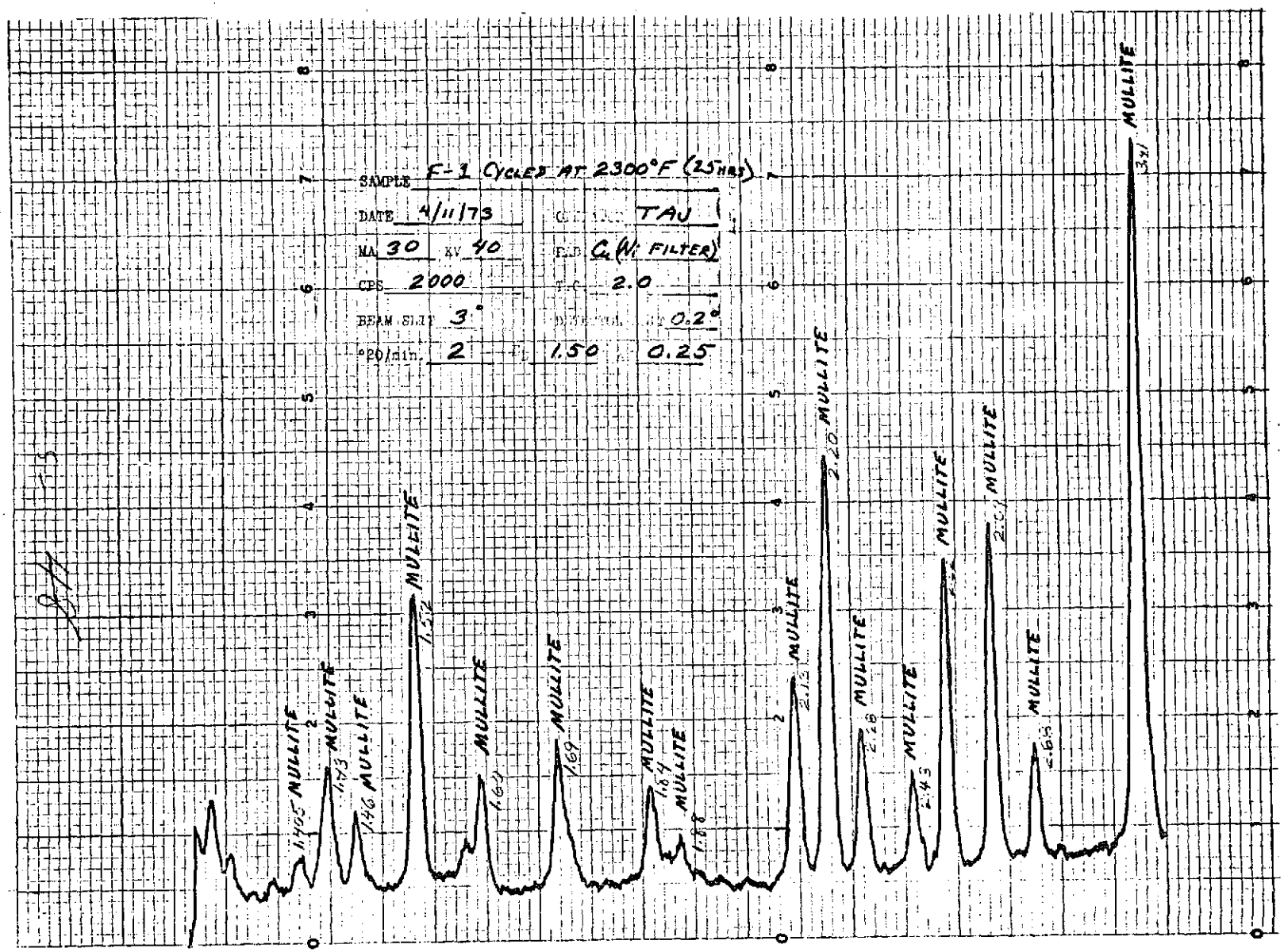

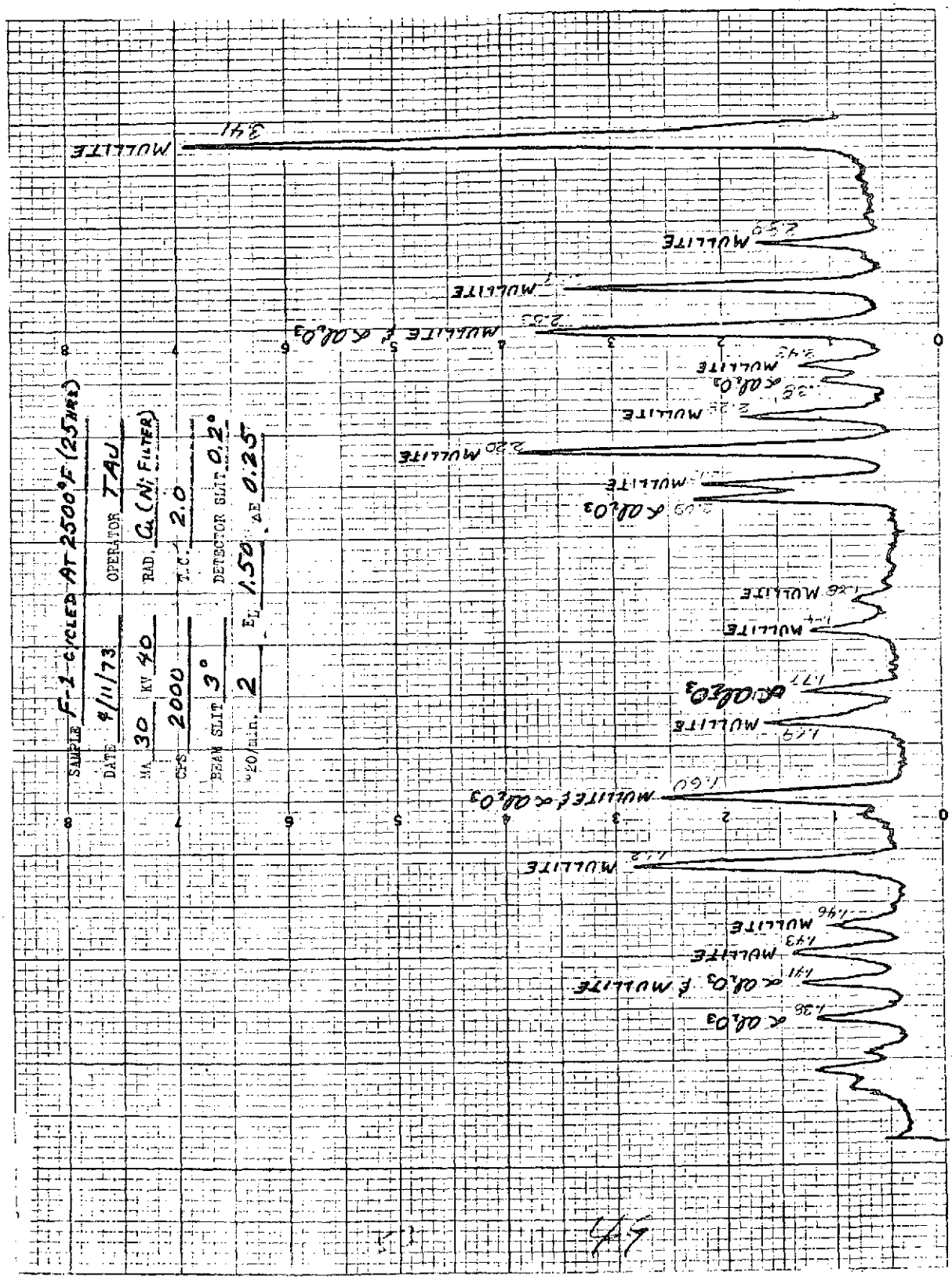

Figure 20. X-Ray Diffraction Pattern of F-1 Fiber After 1371C Thermal Cycling

Figure 21. SEM Examination of F-4 and F-1 Fiber Pads With Binder Before Thermal Exposure

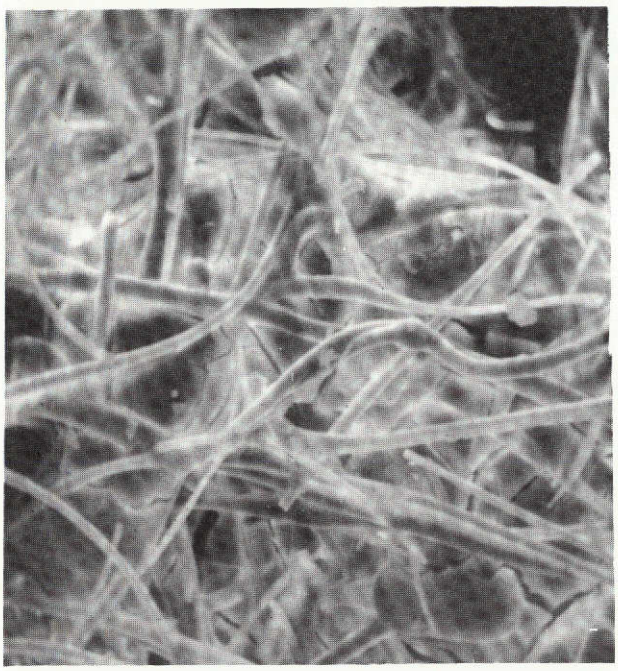

Surface, F-4 Fiber 600X

Center, F-4 Fiber 600X

Surface, F-1 Fiber 600X

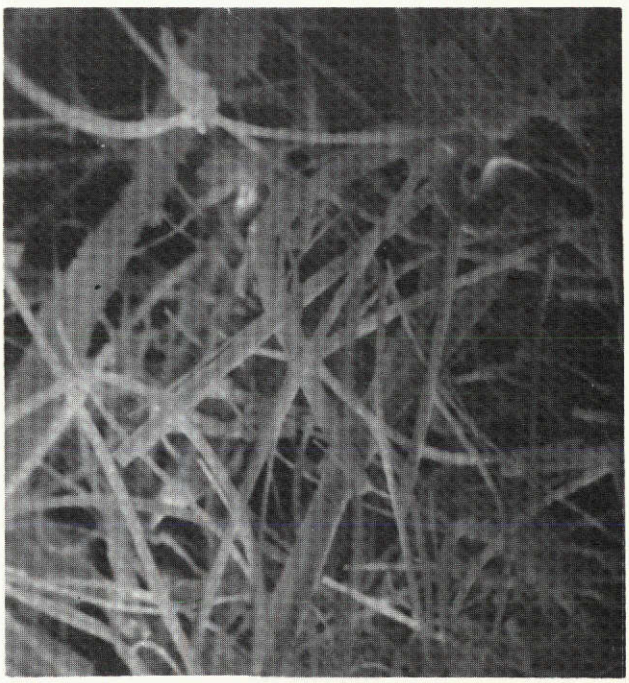

Center, F-1 Fiber 600X

This page is reproduced at the back of the report by a different reproduction method to provide better detail.

Figure 22 shows these pads after exposure to 1259C thermal cycling. There is no visible change in the characteristics of the fiber or the pad. Figure 23 shows the F4 series pads after 1371C thermal cycling. There seems to be no marked degree of change in the appearance of the fiber following the 1371C thermal exposure.

Pads with binder that had been exposed to 1259C were subsequently cycled to 1480C, held for 1 hour, and removed from the furnace. The diametral shrinkage ranged from 0.8 to 2.1%. The shrinkage in height ranged from 0.3 to 2.1%. These pads were then exposed at 1535C for 1 hour. The total accumulated diametral shrinkage for the 1480C and the 1535C exposures ranged from 2.5 to 3.9% for the three pads measured. The shrinkage in height ranged from 2.8 to 5.4%.

These values indicate a degree of stability far in excess of 1371C, which is the goal of this contract. By working to optimize the binder system, a 1480C fiber system appears feasible for the mullite fiber.

4.4 Ten-Pound Mullite Fiber Lot

The best combination of parameters was selected after the evaluations of the thermally exposed fiber pads were completed. Since there was no significant difference in the performance of the F1 and F4 fiber during thermal exposure, fiber F4 was selected as the best process variable combination to use in the manufacture of the 10-pound lot of mullite fiber. This lot was subdivided into 1- and 2-pound packages and delivered to sources for their evaluation as specified by the NASA project manager. The fiber was produced under the following conditions:

Turns open	1/2
Nozzle press., psi	32
Viscosity, poise	10
Rate, g/h	300
Air temp., F	85-100
Rel. humidity, %	22-29

The chemical analysis (wt %) of this 10-pound lot is as follows:

Al_2O_3, 77.6; SiO_2, 16.9; B_2O_3, 5.1; P_2O_5, 1.7

The cross-section of the fiber, as revealed by the transmission electron microscope, is shown in Figure 24. Although x-ray diffraction indicates that a mullite crystalline phase is present, the size of the crystallite is so fine that grain boundaries are not visible.

The production and distribution of the 10-pound lot of blown mullite fiber completed the effort in Task I. Task I demonstrated that the B&W Blowing Process produced mullite fiber with an average fiber diameter of less than 2 microns. The chemistry and dimensional stability of the blown mullite fiber are equivalent to the spun B&W mullite fiber.

Figure 22. F-4 Fiber Pads With and Without Binder After 1259C (2300F) Thermal Cycling

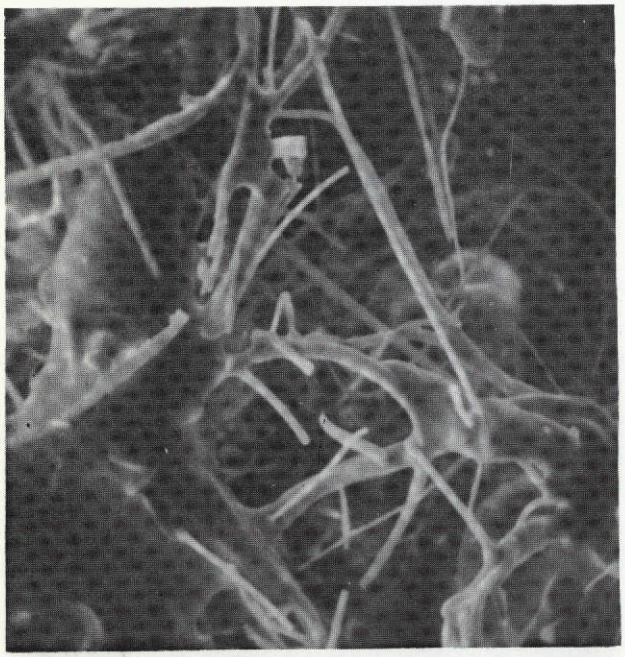

Surface, With Binder 600X

Center, Without Binder 600X

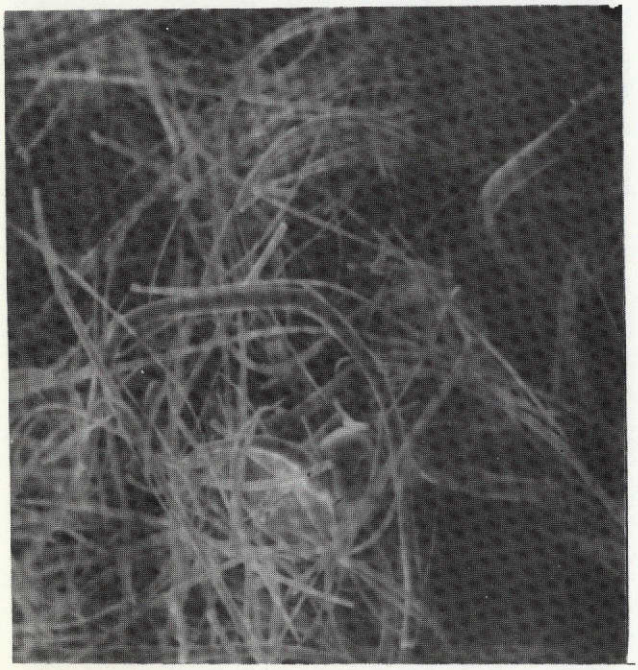

Surface, Without Binder 600X

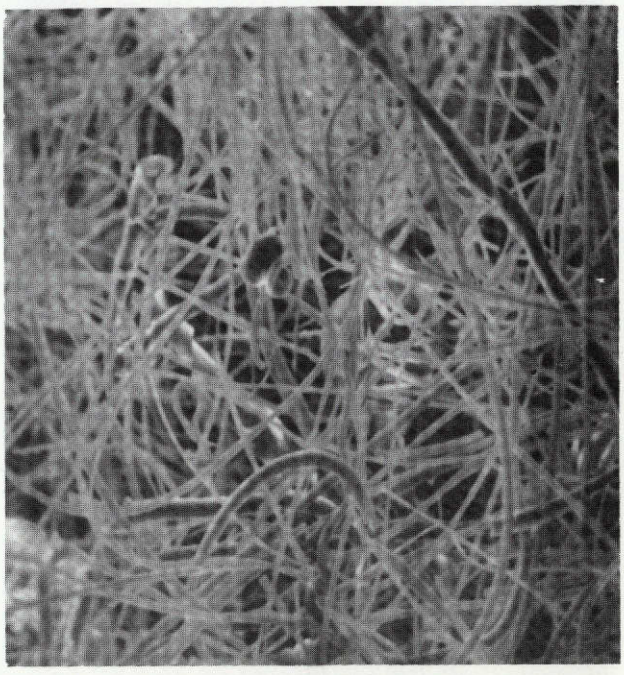

Center, With Binder 600X

This page is reproduced at the back of the report by a different reproduction method to provide better detail.

Figure 23. F-4 Fiber Pads With and Without Binder After 1371C (2500F) Thermal Cycling

Surface, With Binder 600X

Center, With Binder 600X

Surface, Without Binder 600X

Center, Without Binder 600X

This page is reproduced at the back of the report by a different reproduction method to provide better detail.

Figure 24. Fiber From 10-Pound Lot Showing No Apparent Crystallinity

18,000X

5. EXPERIMENTAL PROCEDURE - TASK II

This task was undertaken to examine the thermal stability of three additives as a substitution for the boron and phorphous additives. The three additives and the amounts chosen for the study are as follows:

CrO_3, wt%	1, 3, 5
LiF, wt%	0.05, 0.10, 0.15
MgO, wt%	0.10, 0.25, 0.50

Magnesia (MgO) has proven to be effective in controlling the grain growth in alumina-silica systems in amounts of less than 0.50 weight percent. Lithium fluoride (LiF) acts as a mineralizer in an alumina-silica system in promoting the conversion to the mullite crystalline phase. Chrome oxide (CrO_3) acts to promote and stabilize the mullite phase. Chrome additions to alumina-silica refractories systems in the amounts shown above have imparted excellent stability at temperatures in excess of 1400C.

These additives were introduced into the standard B&W mullite composition in place of part or all of the B_2O_3 and the P_2O_5, and the fiber was blown on the same laboratory apparatus as in Task I.

All of the blown bulk fiber for the additive study was manufactured at the following variable settings:

Nozzle, turns open	1/2
Nozzle press., psig	32
Solution visc., poise	10
Fiber prod. rate, lb/hr	.66
Rel. humidity, %	<25
Room temp., F	75-85

These parameters were determined to be optimum in Task I of the project. At these settings, no difficulty was experienced in blowing the fiber from the additive chemistries.

Pads measuring 2 inches in diameter and approximately 1 inch in thickness were made with a colloidal silica binder from each of the nine additive combinations. These pads were thermal cycled 25 times to 1259C and 1371C by inserting the pads into the furnace, which was maintained at the control temperature. The pads were allowed to remain at temperature for 1 hour and then removed and allowed to cool to approximately room temperature. This process was repeated 25 times at each temperature.

Chemical analyses were performed on the as-manufactured fiber and again following the thermal cycling programs. The MgO was analyzed by spectrographic techniques, the LiF was determined by atomic absorption, and the CrO_3 was analyzed by wet chemical techniques.

X-ray diffraction patterns were produced on each of the nine individual fiber compositions following thermal cycling to 1259C and 1371C.

Electron microscope examination of fiber surfaces and fiber cross-sections were performed on both the scanning electron microscope and the transmission electron microscope. This examination was performed to compare the effects of the different additives on the surface morphology and the grain size in the blown mullite fiber.

Monofilament mullite fiber was extruded, dried, and fired at 1065C for each of the nine additive fiber compositions studied. The fiber was extruded through a single orifice spinnerette.

6. RESULTS AND DISCUSSION - TASK II

Solutions were prepared of each of the nine fiber compositions. With the boron and phosphorous removed, difficulty was experienced with solution stability for each of the additive compositions. The boron and phosphorous impart stability to the mullite fiber solution whereby the viscosity and chemistry of the solution remain stable for at least several days. In this program, the removal of all of the boron and phosphorous from the standard mullite composition rendered the solution viscosity completely unstable. In addition, a precipitate was formed in the 1 and 3 weight percent CrO_3 solutions, as well as in each of the LiF solutions.

To counteract these conditions, the P_2O_5 additive was made a part of the solution chemistry for each of the additive fiber solutions. Previous work (reference 1) had shown that P_2O_5 was more thermally stable than the B_2O_3. Therefore, 1 percent of P_2O_5 was added to each of the CrO_3, LiF, and MgO additive batches, and both the viscosity and precipitate problems were solved.

The 2 inch diameter pads were thermal cycled to 1259C and 1371C to define the dimensional stability of the fiber. A separate group of pads were fired at each temperature.

The results for the 1259C thermal cycling are given in Table 15. In general, the shrinkages are higher than are experienced with standard B&W mullite fiber. Duplicate tests were performed to gain greater confidence in the thermal shrinkage data. The numbers in parentheses in Table 15 are the results of the duplicate testing. In most cases, the high shrinkage values were repeated.

The 1371C thermal cycling results are given in Table 16. Both the 5 wt % CrO_3 pads and the 0.15 wt % LiF pads demonstrated greater dimensional stability at 1371C than at 1259C. Of all the additives examined, the 5 wt % CrO_3 appears to have the greatest dimensional stability after twenty-five 1 hour cycles at 1371C. The 0.15 wt % LiF appears to be the next best selection, but its thermal stability does not compare with that of the standard blown mullite as presented in Tables 18 and 19.

Table 15. Dimensional Stability Following Thermal Cycling of 2-Inch-Diameter Fiber Pads to 1259C

Sample	Diameter change, %		Height change, %	
1% CrO_3	3.6	(8.1)	7.7	(2.5)
3% CrO_3	3.7		7.9	
5% CrO_3	5.2	(5.8)	11.5	(6.5)
0.05% LiF	5.8	(2.0)	7.0	(7.2)
0.10% LiF	4.4	(4.5)	9.4	(5.8)
0.15% LiF	8.6		14.5	
0.10% MgO	3.1		5.6	
0.25% MgO	3.5	(3.0)	9.3	(3.5)
0.50% MgO	2.4	(4.4)	5.5	(5.5)

NOTE: Numbers in parenthesis are shrinkage values taken from a second set of thermally cycled pads to verify results

Table 16. Dimensional Stability Following Thermal Cycling of 2-Inch-Diameter Pads to 1371C

Sample	Diameter change, %	Height change, %
1% CrO_3	1.8	8.0
3% CrO_3	2.6	15.4
5% CrO_3	+1.3	+1.3
0.05% LiF	1.9	12.2
0.10% LiF	3.1	13.3
0.15% LiF	1.1	5.0
0.10% MgO	1.2	13.4
0.25% MgO	2.0	12.0
0.50% MgO	3.0	6.4

NOTE: All numbers are shrinkage except for the 5% CrO_3 samples.

To further evaluate the thermal stability of several fiber pads, thermal cycling was performed to 1427C. The results of the dimensional stability measurements are given in Table 17. The 5 wt % CrO_3 pads produced excellent thermal stability after five thermal cycles, and this composition appears to have potential as a high temperature mullite fiber composition. Additional efforts with the 5 wt % CrO_3 mullite fiber appear warranted.

Table 18 shows the results of chemical analyses of the nine fiber additives as-manufactured, after 1259C, and after 1371C thermal cycling. The MgO was found to be the most thermally stable additive. The results show no loss of MgO at 1371C after 25 cycles. The CrO_3 is the next most stable additive, heaving displayed a loss of approximately 16% after 25 hours at 1371C. The LiF proved to offer little improvement over the B_2O_3 additive in volatility.

Based on the thermal shrinkage results and the relative additive stability, the 5 wt % CrO_3 additive appears most satisfactory to replace the B_2O_3 in the standard mullite composition.

The x-ray diffraction results for the thermally exposed fiber pads are summarized in Table 19. Mullite crystal structure is, or course, the predominant phase, but alpha-alumina is present in many of the fiber pads, especially those that were exposed to 1371C.

There appears to be a relationship between the presence of alpha-alumina and shrinkage at 1371C. The two systems that displayed the lowest thermal shrinkage, the 5 wt % CrO_3 and the 0.15 wt % LiF systems, also displayed only a trace formation of alpha-alumina. The 1 wt % CrO_3 fiber shows no other phase than mullite at both exposure temperatures, but shows greater shrinkage than the 5 wt % CrO_3 or the 0.15 wt % LiF fibers.

The theoretical densities of the several phases present in the mullite fiber are as follows:

	Crystalline phase	Theoretical density, g/cc
As-manufactured (unfired)	Amorphous	2.60
Fired at 1065C	Mullite	3.24
	Gamma-alumina	3.65
Fired at 1259C	Mullite	3.24
Fired at 1371C	Mullite	3.24
	Alpha-alumina	3.98

Table 17. Dimensional Stability Following Thermal Cycling of 2-Inch-Diameter Fiber Pads to 1427C

Sample	Diameter change, %	Height change, %
3% CrO_3	4.5	12.1
5% CrO_3	1.9	2.6
0.05% LiF	3.9	11.8
0.15% LiF	3.3	7.8
0.1% MgO	2.1	8.6

Table 18. Chemical Stability of Additives in Mullite Fiber Composition

Description	CrO_3, wt %
As-manufactured fiber, nominal 1% CrO_3	0.66
1% CrO_3 fiber cycled to 1259C	0.53
1% CrO_3 fiber cycled to 1371C	0.40
As-manufactured fiber, nominal 3% CrO_3	2.72
3% CrO_3 fiber cycled to 1259C	2.24
3% CrO_3 fiber cycled to 1371C	2.11
As-manufactured fiber, nominal 5% CrO_3	4.36
5% CrO_3 fiber cycled to 1259C	4.09
5% CrO_3 fiber cycled to 1371C	3.63
	MgO, wt %
As-manufactured fiber, nominal 0.1% MgO	0.10
0.1% MgO fiber cycled to 1259C	0.10
0.1% MgO fiber cycled to 1371C	0.10
As-manufactured fiber, nominal 0.25% MgO	0.27
0.25% MgO fiber cycled to 1259C	0.27
0.25% MgO fiber cycled to 1371C	0.26
As-manufactured fiber, nominal 0.50 MgO	0.44
0.50% MgO fiber cycled to 1259C	0.46
0.50% MgO fiber cycled to 1371C	0.45
	LiF, wt %
As-manufactured fiber, nominal 0.05 LiF	0.068
0.05% LiF fiber cycled to 1259C	0.054
0.05% LiF fiber cycled to 1371C	0.036
As-manufactured fiber, nominal 0.10% LiF	0.115
0.10% LiF fiber cycled to 1259C	0.077
0.10% LiF fiber cycled to 1371C	0.043
As-manufactured fiber, nominal 0.15% LiF	0.147
0.15% LiF fiber cycled to 1259C	0.108
0.15% LiF fiber cycled to 1371C	0.086

Table 19. Crystalline Phases in Additive Fiber Following Thermal Exposure

Fiber pad	Exposure temp., C	Crystalline phase formed
0.1% MgO	1259	Mullite
	1371	Mullite, with trace alpha-alumina
0.25% MgO	1259	Mullite
	1371	Mullite, with prominent alpha-alumina
0.50% MgO	1259	Mullite
	1371	Mullite, with prominent alpha-alumina
1% CrO_3	1259	Mullite
	1371	Mullite
3% CrO_3	1259	Mullite
	1371	Mullite, with prominent alpha-alumina
5% CrO_3	1259	Mullite
	1371	Mullite, with trace alpha-alumina
0.5% LiF	1259	Mullite
	1371	Mullite, with prominent alpha-alumina
0.10% LiF	1259	Mullite, with trace alpha-alumina
	1371	Mullite, with prominent alpha-alumina
0.15% LiF	1259	Mullite
	1371	Mullite, with trace alpha-alumina

Based upon the densities of the phases shown to be present in the mullite fiber, an increase in alpha alumina formation should produce greater shrinkage. Those fiber samples in Table 19 with the prominent alpha alumina phases formed also had high thermal shrinkage. Stability of the mullite phase, which is formed after firing to 1065C, should retard shrinkage based upon fiber densification. In earlier work (reference 1) the alpha alumina was not developed in the standard mullite composition at 1325C, but was present after thermal cycling to 1450C.

Boron tends to retard the formation of alpha alumina in the standard mullite composition. As boron volatilizes, alpha alumina appears. In the additive fiber compositions studied, the 1 and 5 percent CrO_3 appear to be most effective in delaying the formation of alpha alumina. The 5 percent CrO_3 also has the lowest shrinkage after 1371C exposure.

Electron microscope examination of the fiber was made before and after thermal cycling exposure. This examination showed the mullite fiber as-manufactured to be very smooth, with a progressive roughening produced as a function of time at temperature. No discernible difference was noted in the fibers examined in this program and in the earlier investigations on mullite fiber (reference 2).

A series of scanning electron microscope photographs is shown in Figures 25, 26 and 27. These photographs show a progressive roughening of the fiber surface with thermal exposure. The surface roughening is caused by grain growth, where one grain grows at the expense of a neighboring grain. Another mechanism which is operative at elevated temperature is thermal etching. This phenomena is the selective attack of thermal energy on high energy areas such as grain boundaries, and is analogous to etching of metals or ceramics at room temperature in solution to delineate grain boundaries.

The 5 weight percent CrO_3 fiber after 1371C exposure is shown in Figure 28. The fiber surface is similar to the fiber shown in Figure 27 after the same thermal treatment.

Since the MgO additive was included in this study to attempt to retard grain growth in the mullite fiber, a comparison of the grain size of this fiber with that of mullite fiber previously examined is in order. Figure 29 shows the grain development in standard mullite fiber after 1425C thermal exposure (reference 2). The grain development shown in Figures 30 and 31 is not significantly different. The two levels of MgO added in the fiber shown in these figures did not effectively reduce grain growth.

It appears that the control of grain growth beyond that shown in Figures 29 through 31 may be very difficult to achieve. The fibers shown in Figures 30 and 31 are approximately 2 to 3 microns in diameter, and an individual grain is less than one-tenth of the diameter. Controlling grain size beyond 0.1 to 0.2 microns may be impossible after 24 hours exposure at 1371C. The real question is whether the fiber appears to function satisfactorily in its intended use. The work reported by Tanzilli indicates that grain growth may not be a significant problem (reference 2) when the fiber is chopped and incorporated into a pad with binder.

Determination of the strengths of the additive chemistry fibers was unsuccessful. The fired monofilament fiber was extremely friable in all cases and difficult to handle. Attempts to test the physical strength were unsuccessful due to fiber friability. Apparently, the boron-phosphorous content in the standard mullite composition contributes to the integrity and handleability of the monofilament fiber. A development program may be required to adjust the properties of the solution so that a monofilament can be extruded and tested.

Figure 25. As-Manufactured Mullite Fiber With 0.05% LiF Added

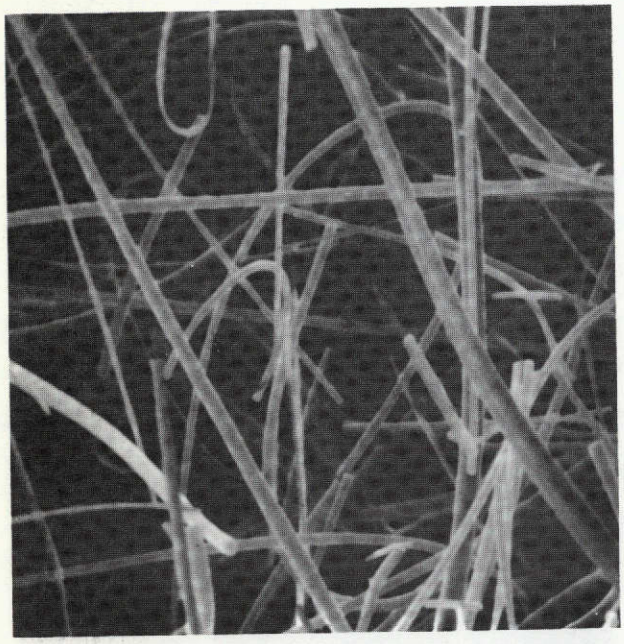

600X

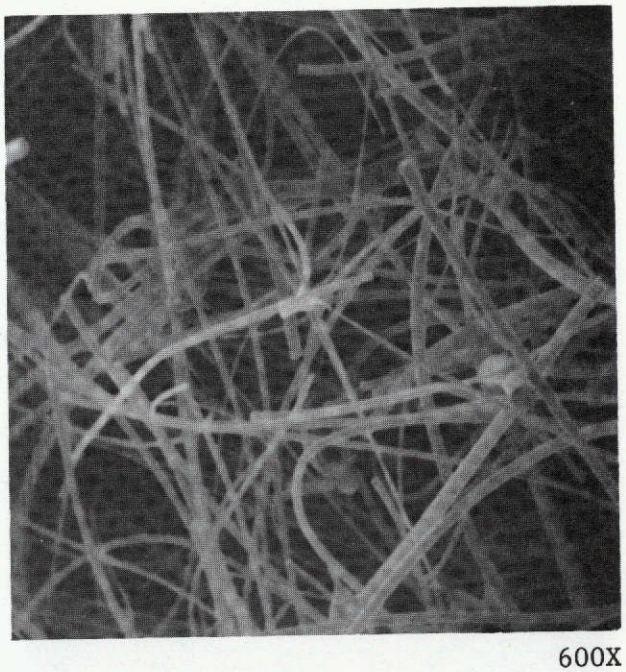

600X

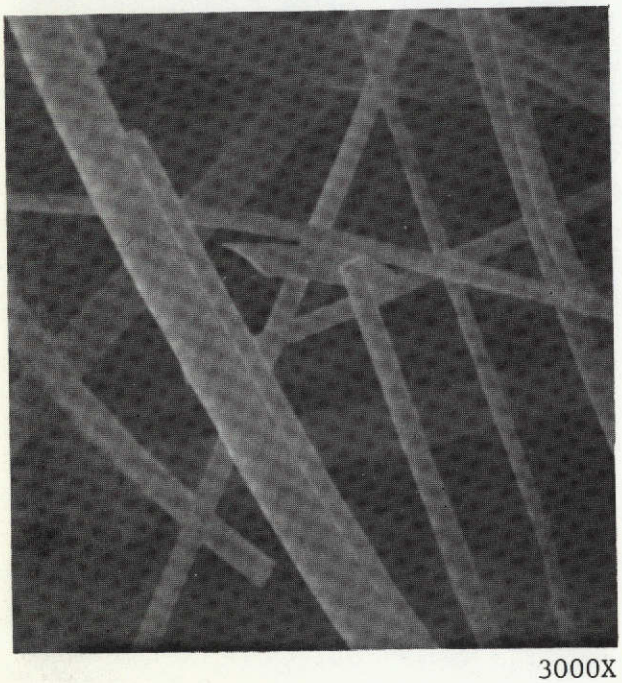

3000X

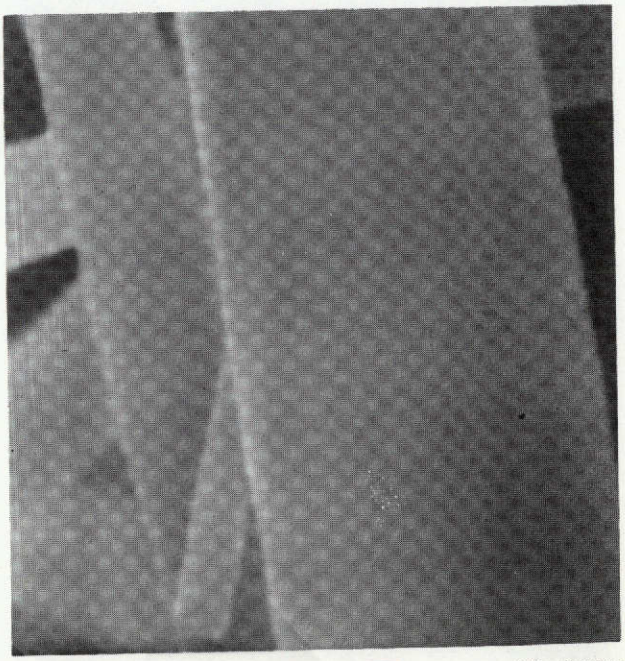

10,800X

This page is reproduced at the back of the report by a different reproduction method to provide better detail.

Figure 26. Mullite Fiber With 0.05% LiF Added, After 1259C Thermal Exposure

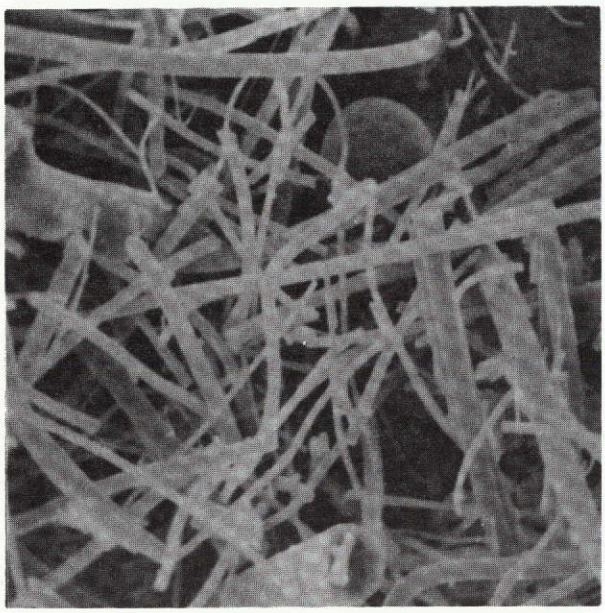

600X

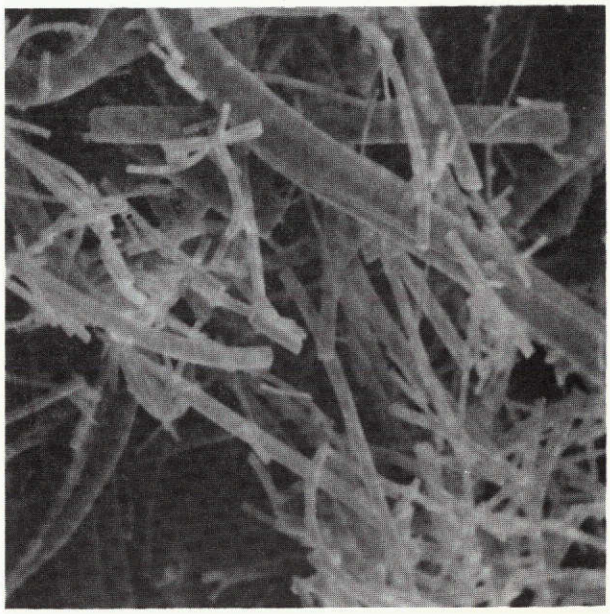

600X

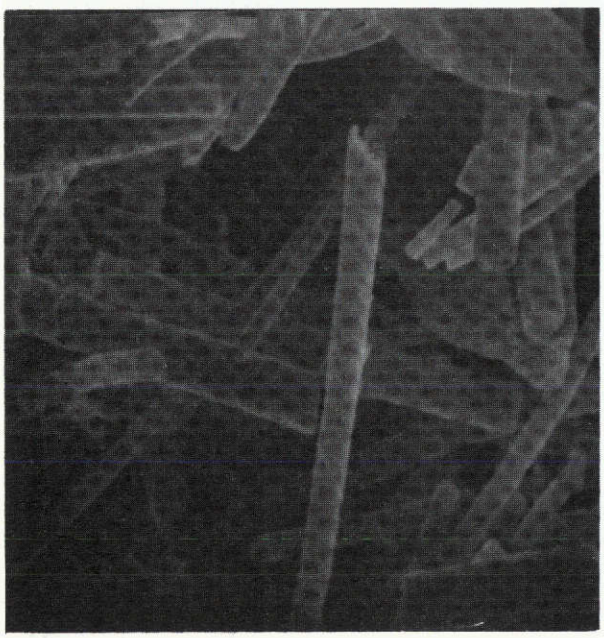

3000X

10,800X

This page is reproduced at the back of the report by a different reproduction method to provide better detail.

Figure 27. Mullite Fiber With 0.05% LiF Added, After 1371C 1371C Thermal Exposure

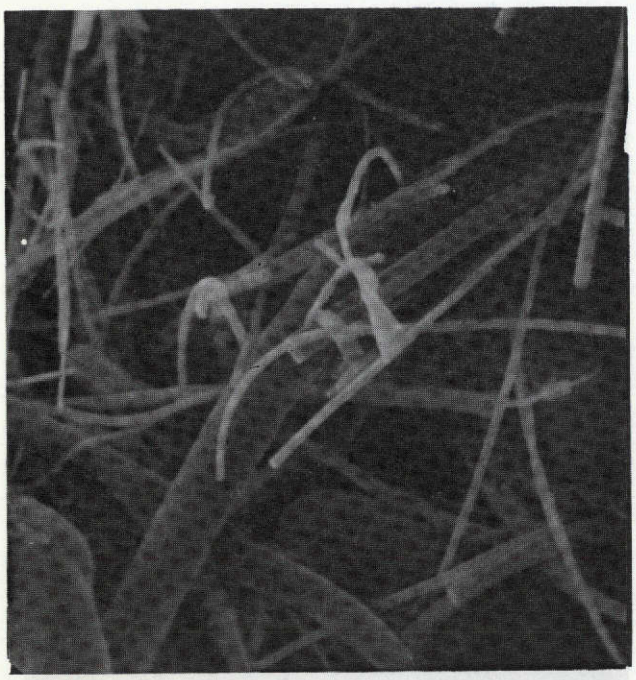

600X

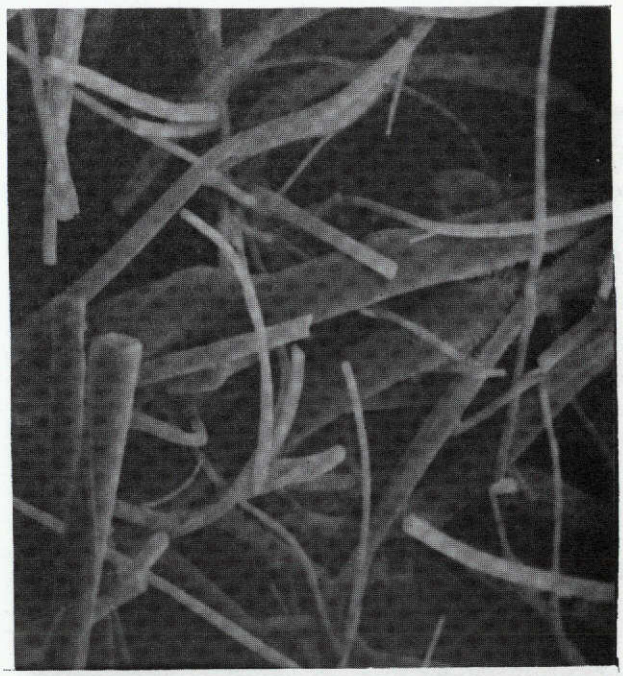

600X

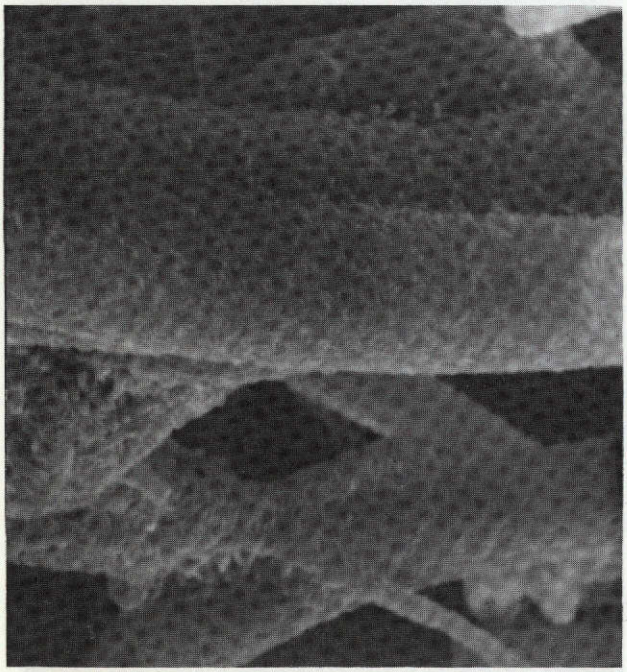

3000X

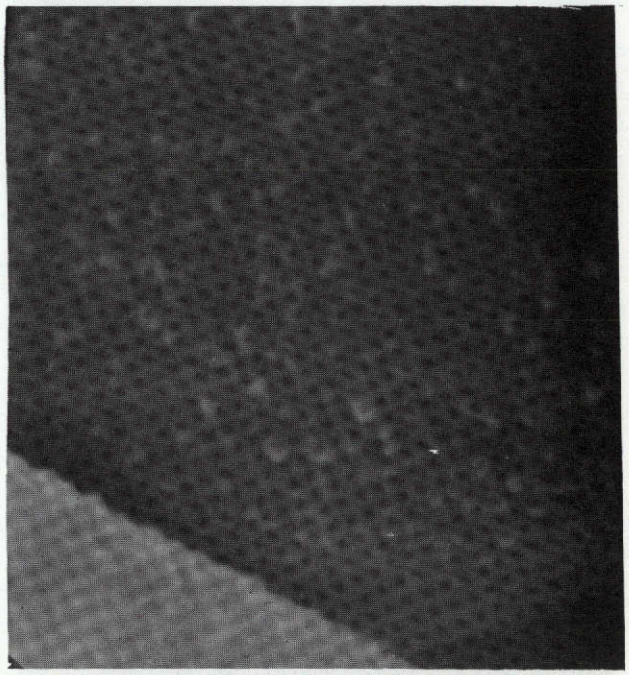

10,800X

This page is reproduced at the back of the report by a different reproduction method to provide better detail.

Figure 28. Mullite Fiber With 5% CrO_3 Added, After 1371C Thermal Exposure

1020X

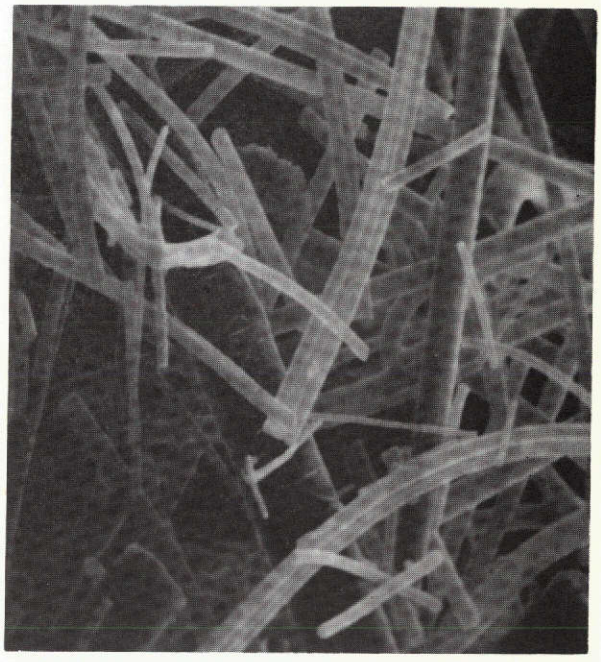

1020X

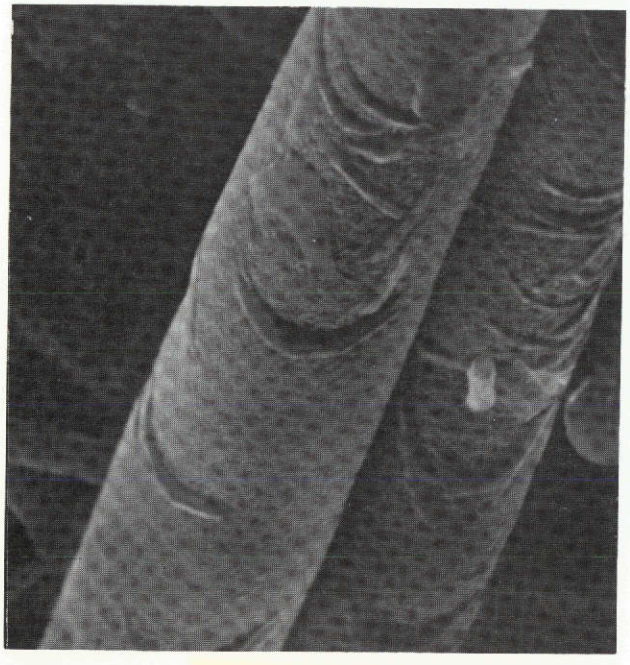

3000X

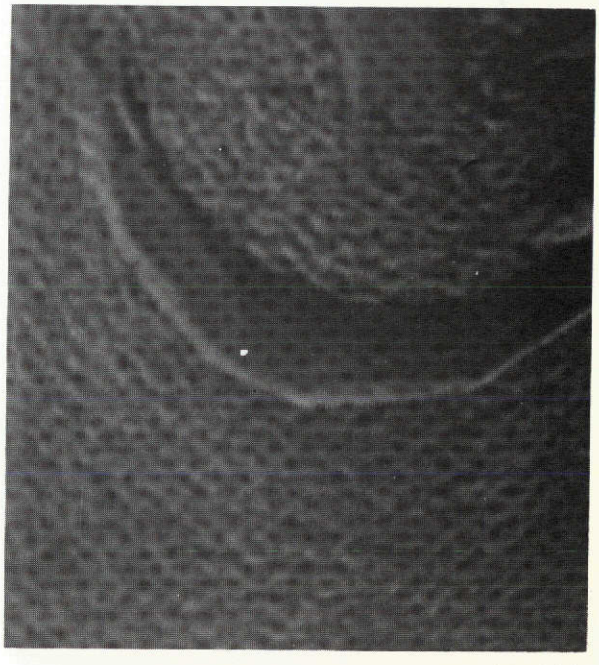

10,800X

This page is reproduced at the back of the report by a different reproduction method to provide better detail.

Figure 29. Mullite Fiber After 1425C Thermal Exposure

Reduced 15% for reproduction. 13,500X

This page is reproduced at the back of the report by a different reproduction method to provide better detail.

Figure 30. Mullite Fiber With 0.10% MgO Added, After 1371C Thermal Exposure

Reduced 20% for reproduction. 15,000X

This page is reproduced at the back of the report by a different reproduction method to provide better detail.

Figure 31. Mullite Fiber With 0.50% MgO Added, After 1371C Thermal Exposure

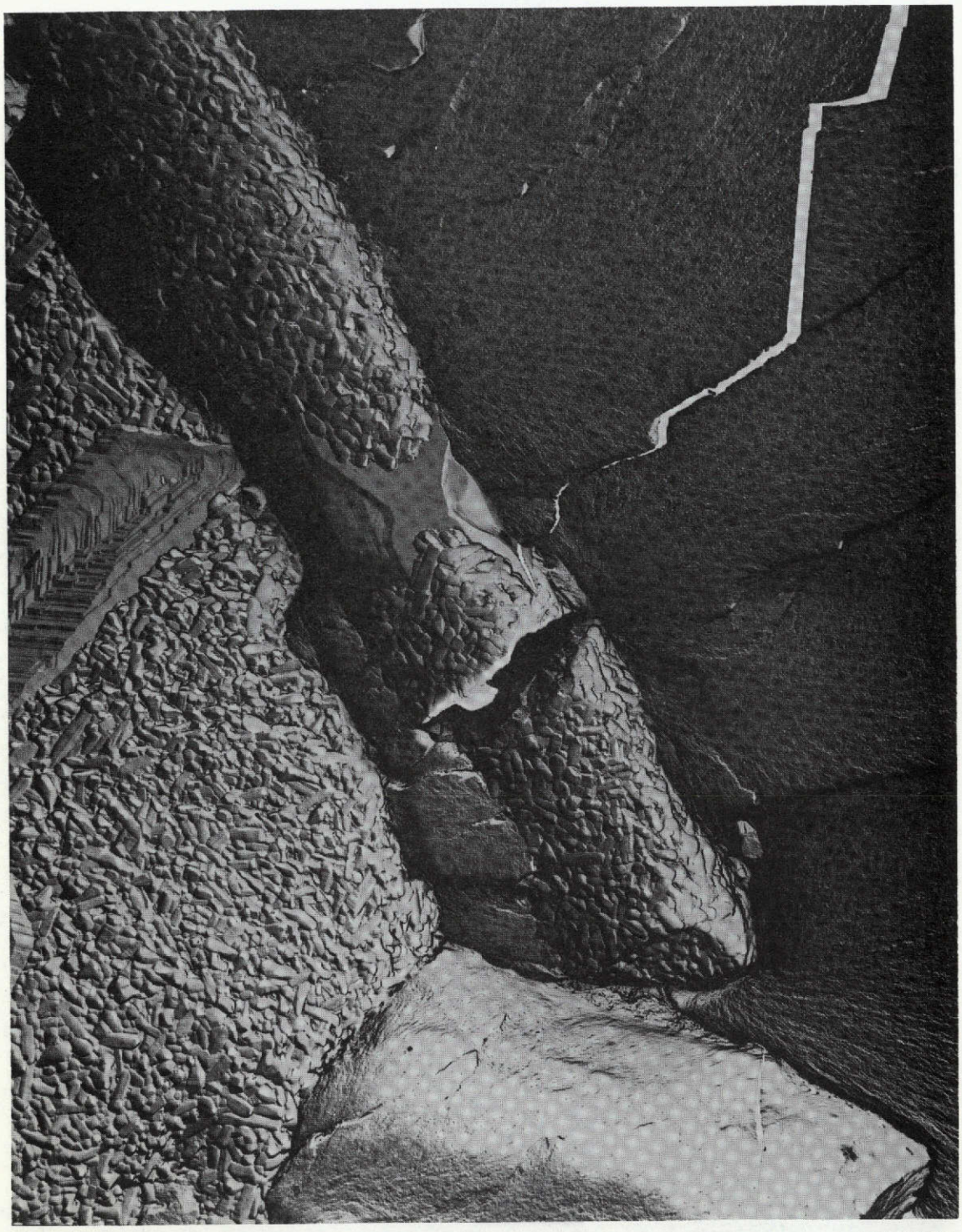

Reduced 20% for reproduction.

15,000X

7. CONCLUSIONS

A program was conducted in two tasks to evaluate fine diameter mullite fiber. Task I involved the production and evaluation of fine diameter (3 microns or less) mullite fiber as produced by the B&W blowing process. This fiber was fully characterized as to fiber diameter distribution, shot size and content, and chemical and dimensional stability in thermal cycling to 1371C. The following conclusions were drawn from Task I:

1. The B&W blowing process produced a mullite fiber that has a significantly finer diameter distribution than does centrifugally spun mullite fiber. Fiber produced by the blowing process has an average diameter of less than two microns, while the spun mullite has an average diameter of approximately five microns.

2. The fine diameter blown mullite fiber (<2μ) produced in Task I has a thermal stability at 1371C equivalent to standard B&W spun mullite fiber.

3. Chemical analyses of as-manufactured, fine diameter blown mullite fiber following thermal exposure to 1259C and 1371C indicate that the chemical stability is equivalent to standard B&W spun mullite fiber.

4. Scale-up of the B&W blowing process from 0.22 to 10 lb/hr was successful. Further work is required to achieve higher production rates, and to refine the parameters for 10 lb/hr production of mullite fiber.

5. The temperature limitations of the mullite fiber have not been defined. Mullite fiber is capable of withstanding temperatures in excess of 1371C.

Task II involved the substitution of CrO_3, LiF, and MgO for the boron additive in the standard B&W mullite fiber composition. The fibers produced were evaluated for chemical and dimensional stability in thermal cycling to 1371C.

The effect of the additives in reducing grain growth was also examined. The conclusions drawn in Task II are as follows:

1. The LiF additive is no less volatile than the B_2O_3. An alpha alumina phase developed at 1259C with LiF may have affected shrinkage. The shrinkage of the LiF additives was high.

2. The CrO_3 additive is not completely stable, but is superior to B_2O_3. The dimensional stability is excellent in fiber pads in the 5 wt % CrO_3 addition.

3. The MgO is extremely nonvolatile at all additive levels after thermal exposure. As a grain growth inhibitor, MgO appears to be as effective as B_2O_3 and is much more thermally stable than B_2O_3.

8. RECOMMENDATIONS

Recommendations for future work are as follows:

1. The temperature limitations of the mullite fiber system should be identified. Based on thermal cycling results from this project, mullite fiber is capable of withstanding temperatures in excess of 1371C. Extending the useful service temperature requires a system consideration - the binder selected must be compatible with the fiber at the desired temperature.

2. Process considerations for fine mullite fiber should be explored. A reduction in fiber diameter requires the development of techniques to properly disperse and locate the binder in a fiber pad. Initial work with the fine diameter mullite as reported in NASA CR-112257 indicates that standard processing techniques used for the larger diameter fiber are not successful for fine diameter mullite. Once the process parameters needed to produce a fine diameter fiber pads are defined, thermal conductivity values should be generated to compare with those of the larger diameter mullite fiber product. Mechanical properties of the fiber tile should be defined at elevated temperatures.

3. The chrome additive fiber composition should be further developed. In addition to its excellent thermal dimensional stability, the chrome imparts a relatively high emittance to the fiber insulation. Earlier research conducted by General Electric under contract[2] to NASA indicates that adding CrO_3 to the coating substantially improves the thermal insulating properties of the fiber block. Blowing process parameters for the chrome additive fiber should be examined in terms of providing the finest possible fiber diameter distribution.

4. Further development of a scaled up fiber blowing system will permit an increased production rate over the current 0.22 lb/hr laboratory rate.

REFERENCES

1. Fetterolf, R. N., "Development Studies on Mullite Fiber," Final Report on Contract NAS3-15564, National Aeronautics and Space Administration, May 1972.

2. Tanzilli, R. A. (editor), "Development of an External Ceramic Insulation for the Space Shuttle Orbiter," NASA CR-112257, National Aeronautics and Space Administration, March 1973.

THE FOLLOWING PAGES ARE DUPLICATES OF ILLUSTRATIONS APPEARING ELSEWHERE IN THIS REPORT. THEY HAVE BEEN REPRODUCED HERE BY A DIFFERENT METHOD TO PROVIDE BETTER DETAIL